An experimental approach to Automatic Exposure Control testing

Rob McLeod

A Thesis submitted for the degree of
Master of Science (Medical Physics)
School of Chemistry and Physics
University of Adelaide
Australia
July 2008

Table of Contents

Abstract

An Experimental Approach to AEC Testing

A New Zealand Qualified Health Physicist (QHP) is required, under the Radiation Protection Act of 1965 and the Radiation Protection Regulations 1982, to perform auditing compliance tests on x-ray equipment at regular intervals to ensure that this equipment conforms to the Code of Safe Practice with the use of x-rays. The protocol for these tests must be approved by the National Radiation Laboratory (NRL).

One of these test protocols sets out the requirements for the functionality testing of the x-ray machine Automatic Exposure Control (AEC). The current NRL protocol for AEC testing is based on the radiographic film environment (NRL C5 1994). This protocol was tested to determine its applicability to the digital computed radiography (CR) imaging systems which are replacing screen-film systems. To begin this process a comparison of the different exposure indexes for each image medium was required. This proved to be achievable using a system of exposure dose comparison. The AEC test process for both image modalities follows identical requirements but differ slightly in the test methods used to achieve these. The most significant finding throughout this stage was not the differences between protocols but was the requirement to achieve consistent exposure index values over the clinical kVp range for each image medium. This requirement, applicable to any x-ray image medium, became the focus of this thesis.

The thesis has explored through experimentation, the effect of optimisation of AEC kVp compensation for the variable kVp response of an image medium, on image consistency. At Christchurch Hospital where this investigation took place the work has shown that the performance of AEC devices can be optimised to improve image consistency, indicated by a more consistent exposure index over the clinical kVp range. The optimisation process also achieves a more consistent dose response to the image plate. A dose variation of 8.3% from the average was achieved compared to 26% in the unoptimised version. No clinically significant changes to image quality were apparent in test images. Under these conditions it was found that AEC functionality could be assessed solely by the measurement of AEC dose to the image plate (IP). Use of this test method provides quantifiable time management benefits for the Medical Physicist and for the radiology departments in which they work.

Disclaimer

To the best of my knowledge and belief this thesis contains no material which has been accepted for the award of any other degree or diploma in any university and contains no material previously published or written by another person except where due reference is made in the text of the thesis.

I give consent to this thesis being made available for photocopying and loan, if accepted for the award of the degree.

Signed:

Acknowledgments

I give thanks to the Canterbury District Health Board for the opportunity and their support to enable me to take part in the MSc program.

This work acknowledges the help of all the people in my work group in the Medical Physics and Bioengineering Department at Christchurch Hospital who have given freely of their time and ideas to aid me in this project.

I also acknowledge the assistance given to me from the radiology staff at Christchurch Hospital who have accommodated me in their work domain during the times when I needed to spend many hours in their x-ray rooms collecting the experimental data required for this thesis.

I thank John Le Heron from NRL in his capacity as my external supervisor for part of my candidature and to Associate Prof Tim Van Doorn and Dr Judith Pollard as principal supervisors and administrative advisers from the University of Adelaide.

I thank the engineering staff of Philips Medical who assisted me in setting up an AEC to conform to the requirements proposed by this thesis.

Chapter 1

Introduction

A New Zealand qualified health physicist (QHP) is required under the Radiation Protection Act of 1965 and the Radiation Protection Regulations 1982, to perform auditing compliance tests on x-ray equipment at regular intervals to ensure that this equipment conforms to the Code of Safe Practice with the use of x-rays. The protocol for these tests must be approved by The National Radiation Laboratory (NRL), a specialist business unit within the Ministry of Health based in Christchurch, New Zealand. NRL provides a resource of expert advice, service provision and research capability on matters concerning public, occupational and medical exposure to radiation, the performance of radiation equipment, and the measurement of radiation and radioactivity. NRL also maintains links to international bodies concerned with radiation protection and associated health issues.

One of the test protocols required by NRL sets out the requirements for testing x-ray machine Automatic Exposure Control (AEC) functionality. The current NRL protocol, NRL C5 section 5.28 to 5.31 in New Zealand, is based on AEC testing in a film environment. With the phasing out of radiographic film and film processors, in the wake of the move into the modern age of digital x-ray detectors and digital image processing, it is an appropriate time to consider the relevance of existing AEC testing protocols (Huda 1997).

AEC devices are designed to automatically terminate an x-ray exposure when their detectors have recorded that sufficient radiation has been received by an image medium to ensure a high quality x-ray image of the subject (Hale 1989). A correctly operating AEC system ensures that consistent imaging quality will result given the same exposure conditions. “As a tool to help ensure correct exposure levels, properly functioning and calibrated automatic exposure control systems may be even more important for Computed Radiography (CR), an example of Digital Radiography (DR), than for film based receptors because there may not be any other technique or stabilising influence as effective as ‘acceptable film optical density’ is for film” (Goldman and Yester 2004).

CR was installed in stages beginning in early 2003 in the radiology department at Christchurch Hospital where the research for this project has taken place. The research for this project was developed using CR imaging technology in order to explore the

appropriateness of current screen-film based AEC functionality testing in a digital imaging environment. This was done with a view to developing a proposal for a new protocol for AEC testing when associated with any imaging medium.

The work for this thesis evolves from a historical view of the development of diagnostic x-ray technology to the development of a procedure to assess AEC functionality using the measurement of dose alone, as described in the following chapter reviews.

Chapter 2 begins with a developmental timeline of x-ray devices and x-ray exposure control. It includes the development of x-ray production and the early understandings of image quality relating to x-ray tube design. Radiation safety issues soon became apparent to the early pioneers of x-ray, with the effects of radiation induced cancers. Radiation safety is an important part of the use of any x-ray devices and underpins much of their developmental work including the use of AECs. This section is followed by the development of x-ray measurements and measurement units used to quantify x-ray dose administered to patients.

The principle of AEC functionality is compared to manual exposure techniques and its advantages highlighted in relation to exposure and image consistency. The components of an AEC system are explained and the chapter concludes with a description of some of the problems that can occur when AEC devices are used incorrectly in the clinical environment.

Chapter 3 describes the standard method of testing AEC functionality in a radiographic film environment. It begins with a description of the film characteristic curve in response to the applied x-ray energy measured in kilo voltage peak (kVp) and presents a typical film optical density (OD) response over the clinical kVp range for a fixed exposure dose. Radiographic film processing is discussed with a focus on the care and handling of the film and the chemicals used in the film development process.

In an attempt to simplify the process of AEC functionality testing and to reduce the time required to perform and assess AEC system performance, a number of test methods and devices have been developed. Some of these, relating to radiographic screen-film imaging, are discussed and evaluated in this chapter.

The final section in this chapter describes how the results of the AEC test procedure are processed and analysed to form the basis of the AEC assessment.

Chapter 4 describes the increasing use of digital technology and lists some of the types of digital devices available for use with digital imaging. Following this is a description of CR technology as an example of a digital imaging system. This leads to a series of sections which details the response of CR with x-rays along with the mechanisms and attributes which are characteristic of CR.

The chapter concludes with a discussion on the implications of using CR in a clinical environment.

Chapter 5 gives a broad overview of AEC functionality in a CR environment. During the initial fact finding process to determine how AEC functions with CR, it was discovered that the CR kVp response was not as consistent as expected. It appears that the reason for this is a generic approach for the AEC set up procedure by the equipment manufacturers. An argument for a more customised approach to this procedure is stated. To maintain image consistency over the clinical kVp range it is important that an AEC should optimally control the dose to the imaging medium according to the kVp response characteristic of the imaging medium. This raised the question of what other benefits could be gained from a protocol which ensures that an AEC is operating optimally.

The chapter is designed to lay out the particular elements of AEC operation within the CR environment. Similar to the procedure for screen-film detailed in chapter 3, the operational dose set-point in the control circuit of an AEC is determined from a requirement to minimise patient dose and to provide maximum imaging information. The parameters used to determine what this dose should be with CR are discussed with respect to the wide exposure latitude characteristic of CR.

The procedure to set the AEC dose set-point with CR at Christchurch Hospital is explained followed by the AEC calibration over the clinical kVp range. The Kodak CR system reports a measure of image contrast assessment with processed images in the form of an ‘exposure index’ (EI). Due to the different parameters used to assess image contrast a method of correlating the exposure requirements for screen-film system OD limits and the Kodak CR EI values was developed. The outcome was an EI variation limit based on existing screen-film exposure parameters. A discussion follows on whether this limit can be improved further with CR.

The chapter continues with a discussion on the use of a standardised x-ray beam for the AEC testing process. Without a beam standard, AEC test results can vary between

different groups performing the same test, which causes confusion when comparing results.

Chapter 6 describes in detail the development of a test procedure to optimise AEC performance in a CR environment. It presents the experimental development processes in a sequential manner, describes the equipment used, outlines problems encountered and presents their solutions. The outcome of these procedures is presented as the test protocol used in the collection of data for this thesis.

In Chapter 7, the results of applying the test procedures developed in chapter 6 are presented here for an AEC with generic kVp compensation applied to match the kVp response of the CR image medium and for an AEC which has been optimally calibrated to match the kVp response of the CR image medium. The dose and EI responses for each AEC setup scenario are evaluated and presented in a graphical format. These are followed by the results of image quality and CR noise testing procedures.

In Chapter 8 the test results for the two AEC test scenarios presented in chapter 7 are comparatively assessed and analysed. It also includes a clinical assessment of images produced under each scenario which will determine any impact on current clinical practice. The introduction of an AEC dose alone measurement as an alternative AEC testing protocol is discussed. This includes the impact of introducing this protocol into a testing program relative to conventional methods and consequently a comparison of test duration for conventional test procedures and the proposed new protocol.

Chapter 9 presents an overview of the thesis. It includes a final summary of the advantages and benefits of implementing this new protocol for AEC testing procedures. Limitations in the practical implementation of this protocol are outlined. The protocol provides procedures to be followed for the measurement of AEC dose alone for the assessment of AEC functionality. This protocol not only simplifies the AEC test procedure but also reduces the total test time required by Medical Physics personnel to perform the necessary tests. The radiology department benefits from this outcome by an increase in the availability of the x-ray machines and CR readers for clinical use. This is shown quantitatively using an experiment which simulates one possible test sequence for an AEC testing procedure.

Future work beyond this thesis is briefly discussed with a view to the application of the protocol to other current CR or DR imaging systems and to new digital imaging systems of the future.

The chapter concludes with the presentation of a proposal to adopt a new protocol for performing the assessment of AEC functionality associated with any x-ray imaging medium using the measurement of AEC dose alone.

Chapter 2

Development of x-ray production and exposure control

2.1 Introduction

Within months of Roentgen's discovery of x-rays in 1895, the phenomenon was utilised for medical purposes to image broken bones and locate foreign bodies embedded in patients. Since then the equipment and techniques employed to produce x-rays have developed to become more efficient, to produce faster imaging times and to improve image contrast and resolution. The modern x-ray machine is designed to be safer to use for both patient and operator.

2.2 The development of x-ray production

X-rays are produced within an evacuated and sealed glass discharge tube or cathode ray tube that has electrodes inserted, to which high voltages are applied. The early cathode ray tubes were not completely evacuated. The residual gas in these tubes was ionised by an electric current and the positive ions produced were attracted to the negatively charged cathode. The collision of these ions with the cathode released electrons that were accelerated toward the positively charged anode by the large potential difference between anode and cathode. When these high-speed electrons struck the anode or target material, x-ray photons were produced. The x-ray photons produced were emitted in all directions. These gaseous tubes were very inefficient, requiring long exposure times to acquire reasonable radiographic images.

In 1913, William Coolidge invented an x-ray tube that featured a high vacuum and used thermionic emission from a heated filament as the source of electrons. The small amount of gas left in this type of tube did not contribute to the production of electrons (Hendee 1979). Other inventions followed including the focussing cup that concentrated the electron production from the filament to a small part of the anode called the focal spot and the line focus design using an angled anode target to create a small focal spot which produced sharper images.

The efficiency of x-ray production was increased with these inventions but as x-ray production increased, so too did the heat production at the anode target of the tube.

Various materials were used for the anode target in order to find a substance that could withstand the heat generated by the electron beam striking the target. As x-ray production increased, the mass of these target materials had to increase to avoid the destruction of the target. Target materials with higher atomic numbers performed best and tungsten with an atomic number of 74 proved to be one of the more preferred materials and remains so today.

In the 1930s the rotating target (anode) x-ray tube was developed. Figure 2.1 is a schematic diagram of a rotating target (tungsten) x-ray tube showing the anode connected to the end of a rotor shaft. This development allowed the target position to change continuously, effectively increasing the area of the target material, enabling greater heat conduction away from the actual target area (Mould 1995). All of these inventions and developments have contributed to the design of modern x-ray tubes.

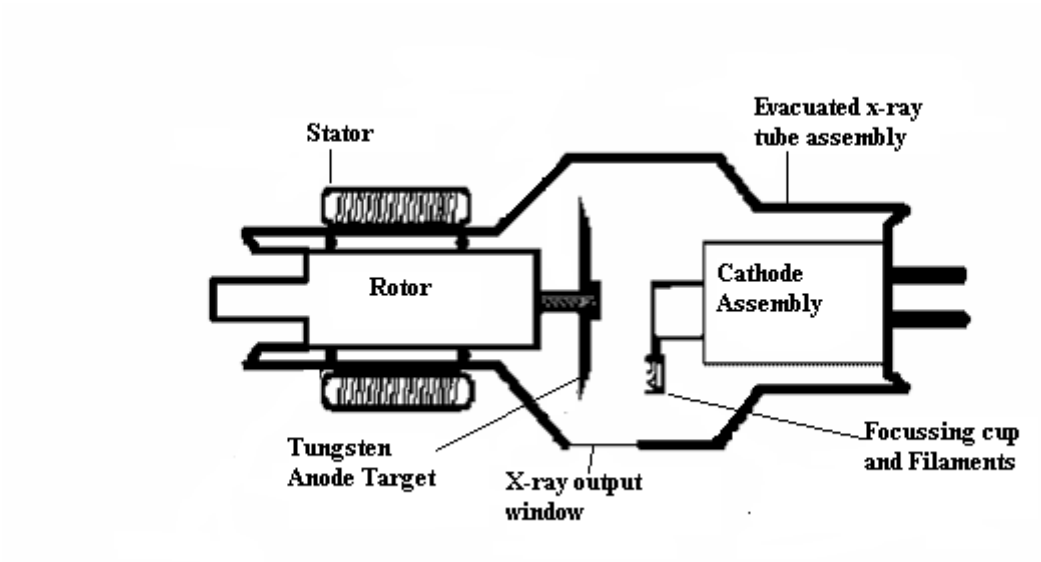

Figure 2.1 The rotating anode x-ray tube with line focus

2.3 X-ray radiation protection

The x-ray photons produced by an x-ray tube are known to cause cellular damage in biological organisms that may lead to the development of cancers. This is due to the effects of ionising radiation on the atomic structure of objects exposed to these x-rays. The x-ray photon is an energetic particle which interacts through collisions with the orbital electrons in this material, thereby losing energy. Ionisation is the process where electrons of the absorbing material are ejected from their molecular structure due to these collisions. These free electrons can further interact with matter and may cause damage to the normal cellular structure, leading to the possibility of cancers. It is

therefore very important to protect both patient and operator from unnecessary x-ray radiation.

The lack of radiation protection to the x-ray operator and to the un-imaged parts of the patient is notable in the early photograph shown in Figure 2.2 of a portable military set up being used by Ernest Harnack. Harnack was one of the first casualties of radiation-induced cancer after the discovery of x-rays.

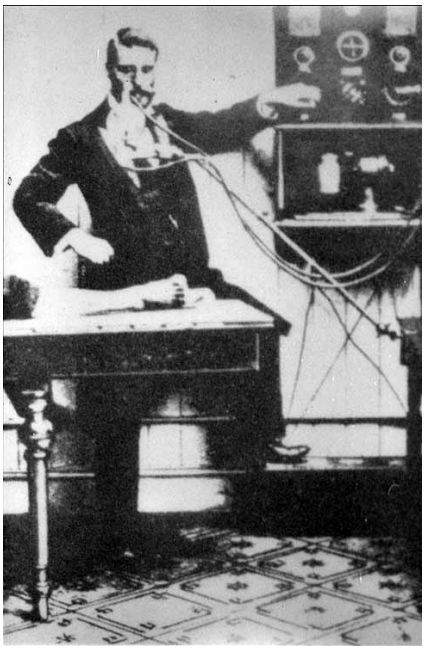

Figure 2.2 Ernest Harnack (around 1896) using a portable military set-up, including a Ruhmkorff coil and early vacuum tube. (Photograph courtesy of the Radiology Museum Brussels, Belgium)

The early x-ray tubes were not encased in radiation protective material, nor did the operators stand behind radiation protective barriers or wear radiation protective apparel, as is the case today. The continued use of these unprotected machines and the lack of external protective barriers caused many cases of radiation-induced medical problems to the early operators. As developments in x-ray machine technology increased, so too did the awareness of the potential for harm from exposure to x-rays. This led to the realisation that operators and patients required greater protection from unnecessary x-ray exposure and that this protection should also include some form of control over the exposures themselves.

The modern x-ray tube is encased in radiation protective material to minimize the emission of unwanted (scattered) x-ray photons. While x-ray photons are emitted from the anode target material in all directions, the modern tube design and construction only allows photons to exit the tube easily through a thin window in the glass envelope. This window is usually made of some material that is highly transmissive to x-rays such as beryllium. The x-rays emitted through this window can then be shaped by collimation to become the directional beam of x-ray photons that we are familiar with today in our x-ray facilities.

2.4 Measurement of x-rays

One of the earliest quality control measurements of x-rays, performed in 1904, was to observe the colour of the glass surface of the x-ray tube, which changed due to fluorescent processes when x-rays were being produced. The type of fluorescence produced under differing conditions indicated how well and in what state the tube was operating. Further quality control measurements were developed over the next few years, including the use of quantitative instruments such as radiochromators, chromoradiometers and quantimeters that were a great improvement over the qualitative visual methods. Figure 2.3 is a photograph of the 'pastille' chromoradiometer. This instrument was developed by Holzknecht in 1902 and provided a measurement of x-ray radiation based on the photochemical effect and the consequent changes in colour of a mixture of sodium carbonate and potassium chloride. Holzknecht evaluated the dose that would produce a mild skin reaction and designated it as 3H. The 'H' unit was widely adopted as a dosimetry measure for decades (Van Loon and Van Tiggelen 2004).

In 1896, J. J Thomson conducted experiments which explained Roentgen's observations of the conductive properties of materials through which x-rays had passed by saying that the radiation 'ionised' the material (Mould 1995). The ability of x-rays to ionise the material through which they passed was exploited to quantify the measurement of x-rays. Of particular interest in the design of instruments developed for this purpose was the gold leaf and tin foil electroscope invented by Abraham Bennet (1750-1799). This utilised the ionising effects of x-ray radiation and could be considered the forerunner to the concept of using a free-in-air ionisation chamber in the measurement of x-ray ionisation. This concept was first expounded by Jean Perrin in 1896 but it was not until the 1920s that practical working models were being produced (Mould 1995).

Figure 2.3 The Holzknecht chromoradiometer scale (Photograph courtesy of the Radiology Museum Brussels, Belgium)

2.4.1 X-ray dose measurement units

A unit based on the measurement of the effects of x-ray ionisation was proposed by Villard in 1908. Villard's e-unit as it was initially called was defined as the liberation of one 'esu' of charge per cc of dry air (the esu or "electrostatic unit" is the cgs unit for electric charge) (Mould 1995). The size of the esu is set so that the constant in Coulomb's force law is equal to one. This law states that two charges each of 1 esu placed 1 cm apart experience a force 1 dyne = 1.0×10^{-5} newtons (N). The magnitude of the charge (e) of an electron is e = 4.8×10^{10} esu. The e-unit as defined above was renamed as the German roentgen (R) unit, which in 1928 at the second international congress of radiation became internationally accepted as a measurement unit for radiation exposure (Van Loon and Van Tiggelen, 2004).

Exposure is defined as the amount of electrical charge produced by ionising radiation per mass of air measured in coulombs per kilogram (C/kg). The traditional unit of exposure is the roentgen which is defined as:

$$1\ R = 2.58 \times 10^{-4}\ C/kg$$

A second unit of radiation quantity, the gray (Gy) was defined in 1979 by the International Commission on Radiation Units and Measurements (ICRU report 33). One gray is equal to the absorbed dose when the energy per unit mass imparted to matter by ionising radiation is one joule per kilogram (J/kg). X-ray exposure is measured using standard air filled ionisation chambers. Exposure is almost proportional to absorbed dose in soft tissue over the diagnostic energy range, typically 10 keV – 150 keV, because the atomic numbers of air and soft tissue are similar (approximately 7.5). The roentgen and the gray are the standard units of measurement used for the test procedures involved in this work. The relationship between these two units in air is (Bushberg et al 2002, pp 54-56):

$$1\ R = 0.00876\ Gy.$$

2.5 The development of exposure timers

Prior to the development of AEC devices, all medical radiographic examinations were performed manually. When the Medical Radiation Technologist (MRT) performs a manual radiographic exposure, the exposure controls of the x-ray machine are set according to the MRT's estimated exposure requirements for the particular anatomical image required.

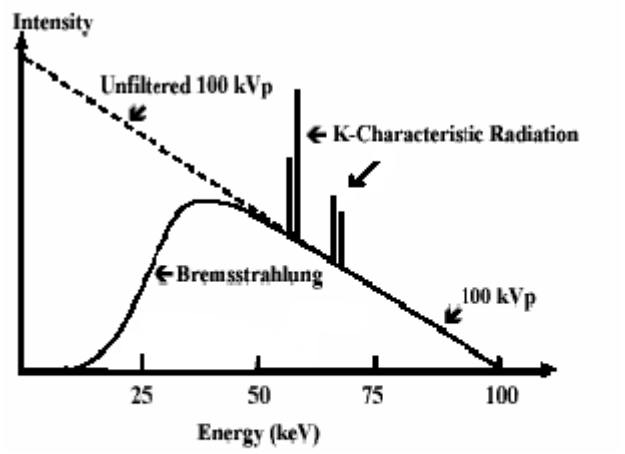

Figure 2.4 X-ray energy spectrum from a tungsten target

The settings made will depend on patient size and pathology. Control of these exposures is achieved by adjustment of the beam energy in kilo voltage peak (kVp),

the x-ray tube current in milliamps (mA) and exposure time in seconds (s). The kVp value gives the maximum photon energy within the spectrum produced by the x-ray tube. The x-ray energy spectrum from a tungsten x-ray target is shown in Figure 2.4 for a 100 kVp exposure. A useful radiographic image is achieved only if all the exposure factors are set optimally to match the exposure conditions. The manual timers used for these exposures were initially controlled mechanically and later electronically. An example of a type of electronic timer uses pulse-counting techniques to accurately control the time of short exposures. The pulses are generated by quartz crystals capable of high frequency modes of operation. A higher degree of timer accuracy is obtained as the crystal's operating frequency is increased (Christensen et al 1990).

The invention of the ionisation chamber during the 1920s was the forerunner to the development of ionisation timer devices for use with AECs to measure and control x-ray exposure time. When used for this purpose the ionisation chamber is located in the x-ray beam and produces a very small electric current (in the order of μA). This current is then used to charge a capacitor in the AEC control circuitry. When this capacitor, used as an electronic storage device, reaches a predetermined charge, the exposure-terminating switch is activated to terminate the exposure.

In the 1940s, under the supervision of Dr Hodges who created a research-oriented department at the University of Chicago, Russell Morgan began work on a phototimer (University of Chicago, Department of Radiology web page, The Early Years 2004). His work was based on principles first appearing in articles in the German literature of the time. The x-ray exposure causes light to be given off by a fluorescing screen placed behind the radiographic film. This light activates a photoreceptor device located in front of the fluorescent screen. The electronic output from this device is applied to a capacitive trigger circuit in a similar manner to the ionisation chamber described previously. A major problem with the low sensitivity of the earlier photoreceptor devices was solved when Morgan used a new photomultiplier tube developed by the Radio Corporation of America (RCA). The first commercial phototimer that used Morgan's invention was marketed by Westinghouse in 1945. Morgan's phototimer was initially designed for use with photo fluorographic devices. These devices include a fluoroscopic x-ray unit and a camera intended to be used to produce and then photograph a fluoroscopic image of the body. A fluoroscopic x-ray unit uses a fluorescing screen to view real time images of patients rather than a single shot fluorographic screen-film technique.

2.6 AEC functionality

The detectors of an AEC are typically ionisation chambers which are located in front of or behind the imaging medium, in Bucky mechanisms as described in section 2.6.1. The complete assembly lies in the primary beam of the x-ray tube. This means that the AEC detectors are subject to the same radiographic conditions that the imaging medium is subject to. The essential elements for all AEC devices are that they detect x-ray radiation, they should not show an image of their structure on the image receptor plate and they should produce a small electric current proportional to the amount of incident radiation which can be used to control exposure timing.

Manual timing techniques terminate an x-ray exposure at a time determined by the estimations of the radiographer to satisfy the clinical requirements of a particular procedure. This can lead to gross under or over exposed radiographs, requiring repeat exposures to obtain precise imaging information. These extra exposures result in increased x-ray dose to patients and increase the occupational radiation risk to radiology staff.

An AEC device provides the ability to consistently control exposures irrespective of the anatomical view, patient size or pathology transited (Mazzocchi et al 2006). The benefits of this consistency include increased operational efficiency, decreased exposure repeat rates and hence decreased exposure to both patient and radiology staff. The ideal AEC should maintain a consistent dose to the image medium within the range of clinically defined operational parameters. Dose consistency also implies that the signal to noise ratio (SNR) should remain constant for images and that image quality is consistent (Doyle 2005).

When an x-ray exposure is controlled using an AEC device, the technologist sets the kVp and tube current as for the manual approach, but the exposure time is controlled by the AEC exposure termination control circuit. This device terminates the exposure only after a preset charge on its capacitive trigger circuit has been reached, indicating that sufficient radiation has reached the imaging medium to produce a quality radiographic image. Figure 2.5 is a simplified schematic diagram of an AEC control circuit. The AEC detectors in this diagram respond to the x-rays emitted by the x-ray tube and produce a small electric current. This current is directed through a buffer amplifier and causes a charge to accumulate on the capacitor at a rate proportional to the amount of radiation present in the x-ray beam. The exposure time is determined by the state of the accumulated charge on this capacitive trigger circuit. When this charge

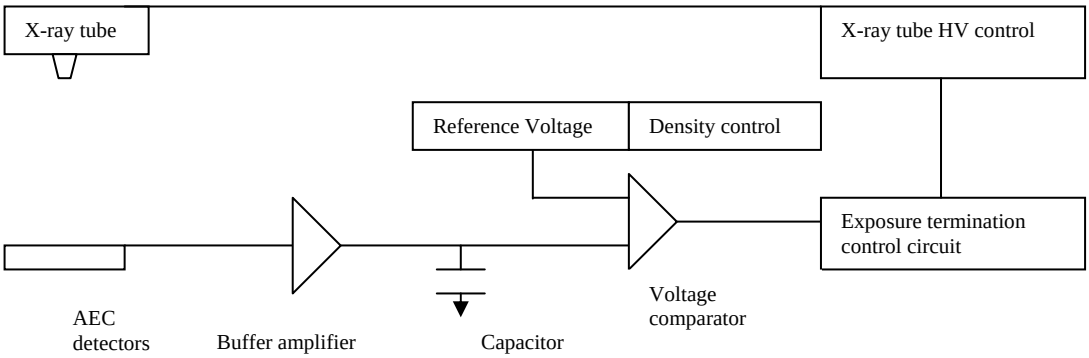

Figure 2.5 AEC control schematic diagram

reaches the preset reference voltage, the voltage comparator output activates the exposure termination control which in turn switches off the high voltage (HV) to the x-ray tube, terminating the exposure. The density control is able to alter the state of the reference voltage up or down to accommodate for extremes of patient size or at the discretion of the radiographer to achieve optimal image quality, whilst maintaining a consistent response over the clinical kVp range.

2.6.1 The arrangement of AEC detectors

The AEC detectors built into modern x-ray machines are located in Bucky assemblies. A Bucky is a mechanical device that supports the anti scatter grid assembly, AEC panel and the drawer assembly that supports the imaging medium in the x-ray beam. Dr Gustave Bucky is recorded in many historical accounts as the person who in 1913 invented the x-ray grid for anti scatter control (Newing 1999). The attributes and function of a Bucky are discussed in section 6.5. Modern x-ray rooms typically have two Bucky arrangements to accommodate a wider range of exposure techniques. The table Bucky is built into the x-ray table structure to enable imaging of patients lying in a prone position, while the erect or chest Bucky can be a stand-alone or wall mounted assembly for imaging patients able to be positioned standing or seated.

A Philips x-ray machine is shown in Figure 2.6. The erect Bucky associated with this machine (photo left centre) shows the position of the three AEC chambers. The x-ray tube and collimator assembly is shown on the right of the photo.

AEC detectors are of two types: entrance detectors are located in front of the film cassette tray; exit detectors are located behind the film cassette tray.

Each AEC chamber is independently selectable by the MRT. A single chamber can be selected or combinations to match the exposure requirements of the anatomical area to be imaged. Some manufacturers apply a differential to the operational sensitivity of the individual AEC chambers. The differentials are designed to match the attenuation coefficients of the main anatomical areas of the lungs, heart and abdomen.

Figure 2.6 X-ray machine erect Bucky (centre left of photo) showing the physical arrangement of the three ionisation chambers used as x-ray detectors for the AEC.

2.7 Incorrect use of AEC procedures

When AEC devices are used to control x-ray exposure in accordance with their design, the images produced should have a consistent image quality. A number of events can occur when applying AEC procedures that can lead to inferior imaging and the probability of repeat exposures. A selection of these events is given below.

Chamber position and selection

Incorrect chamber selection relative to the patient anatomy to be imaged will cause inferior imaging results. While some Buckys are clearly labelled with the position of their AEC chambers, others have only a thumbnail drawing of the layout, as shown in Figure 2.7 applied near the Bucky tray. This may show the orientation but not the actual size and position of the chambers themselves relative to a patient's anatomy. As a result, the selection of AEC chamber or chambers relative to the required anatomical

area of a patient can be erroneous. The effects of this type of exposure inaccuracy may be a total or partial exclusion of the selected AEC chamber from the primary x-ray beam especially where close collimation is required. In this type of situation the AEC will prolong the exposure until it records that sufficient dose has been collected or it reaches its exposure safety limit. The result will be an over exposed image and a higher exposure dose to the patient. The exposure may have to be repeated after correcting the exposure setup, resulting in further dose to the patient.

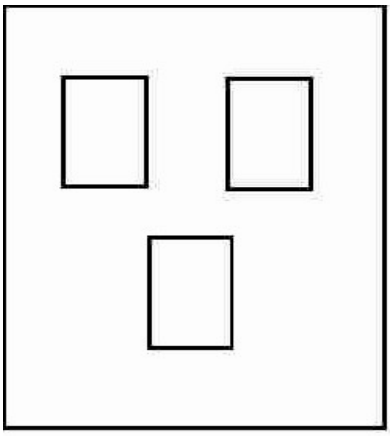

Figure 2.7 Standard AEC 3 chamber thumbnail layout

Paediatric patients

The standard physical AEC chamber layout presents problems for paediatric radiography. The physical size of the paediatric patient relative to the size and position of the standard AEC chambers can lead to positional errors or exposure timing problems similar to those discussed above.

KVp selection

The correct selection of kVp is a critical factor for image quality and minimising patient dose. For example, if an inappropriately low kVp technique is set for a large patient, the AEC will attempt to maintain the exposure until its programmed trigger dose has been reached. However it may not achieve this point before the maximum safe exposure time has been reached at which point the AEC terminates the exposure. The result again will be poor image quality and unnecessary dose to the patient. The exposure would need to be repeated at a more appropriate kVp setting, resulting in further dose to the patient.

The use of Computed Radiology (CR) as the imaging medium with AEC

When CR technology is used as the imaging medium, the radiographic techniques must be closely monitored to ensure that the wide dynamic range of CR and post processing methods do not hide inefficient or inappropriate radiographic technique.

There are many benefits to be gained from the use of AEC devices. However, as indicated by the problems highlighted above, the use of an AEC device does not relieve the operator of the responsibility of using good quality radiographic techniques.

Chapter 3

AEC in a screen-film environment

3.1 Introduction

AEC functionality in any imaging environment is assessed by testing the following radiographic parameters: reproducibility, detector chamber response, kVp response, patient thickness response determined using a patient equivalent phantom (PEP), density control function and the maximum and minimum x-ray exposure times. The focus of this thesis is on the AEC response to varying kVp and PEP thickness for the particular image medium for which the AEC is calibrated. For the screen-film imaging medium, this is achieved by recording and analysing the optical density (OD) of the radiographic film images resulting from a range of test exposure conditions.

The OD is a unit-less index of radiographic film darkening measured by a densitometer instrument. This instrument measures the light transmittance through radiographic film images. It displays the result on a logarithmic scale which matches the response characteristic of the human eye. The use of such a scale allows large OD variations to be displayed on a small scale and also allows OD combinations to be additive.

The AEC is expected to control the exposure time of x-ray procedures in order to produce consistent image quality over the range of clinical kVp and patient thickness. By recording the OD of homogenous images produced under different conditions of kVp and patient thickness, a profile of the uniformity of the AEC function is obtained. Any variations in this performance over the test exposure conditions must fall within specified tolerance limits to conform to quality assurance requirements. Should the AEC performance vary beyond these requirements then the problem causing the erroneous AEC behaviour must be corrected by the service engineers.

3.2 The screen-film imaging system

Radiographic films have poor sensitivity to direct x-ray radiation and their use would result in large exposures to patients in order to obtain a reasonable image. Consequently, most radiographic procedures use luminescent screens, which convert the radiographic image to light (fluorescence). The film is most sensitive to this fluorescence and it is this radiation that forms the latent image on it. The screens are a

permanent part of the internal structure of a typical x-ray film cassette into which the radiographic film is placed. Because of this, I will refer to radiographic film as screen-film in future references to this image medium, unless the film itself is the subject of the reference.

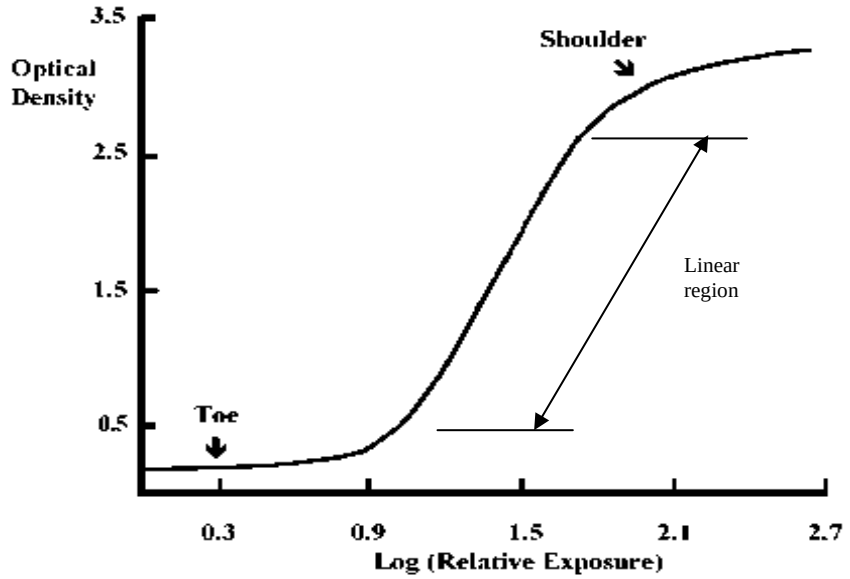

Figure 3.1 Typical screen-film characteristic curve (H&D curve)

The combination of a luminescent screen with radiographic film reduces patient dose, x-ray generator loading, exposure duration and hence patient motion artefacts (Heggie et al 2001). This is due to greater x-ray detection efficiency of the luminescent screen compared to the radiographic film by itself. Screen-film combinations are considered to be contrast limited in their response because their range of lineal contrast changes with exposure is relatively small (Christodoulou et al 2000).

A typical characteristic curve for screen-film of the type originally published by Hurter and Driffield (H & D curve) in 1890 is shown in Figure 3.1(Bushberg 2002). It plots film optical density against the logarithm of the exposure at a particular kVp. The shape of the curve and the slope of the linear region vary for different screen-film types. The contrast performance of the film image is related to the slope of the curve as this characteristic determines how fast the film density changes with different exposures. A steeper gradient of the curve corresponds to greater change in film density for the same variation of exposure dose.

The sensitivity of screen-film combinations varies with kVp as shown in the experimental results plotted in Figure 3.2. The graph shows the response of a Kodak T - Mat-G-RA screen-film system exposed to a fixed dose of 0.8 mR over the kVp range 50 kVp to 125 kVp. For each plotted kVp value on this graph, exposures were performed by adjusting the x-ray source to image distance (SID), tube current and exposure time to achieve 0.8 mR at the plane of the image medium placed in a Bucky tray. This graph is presented not to show absolute OD values at each kVp but rather to obtain an understanding of the shape of the response for this medium, especially at the lower end of this range (50 to 70 kVp). The results show that the response is poor at the lower end of this kVp range and then steadily increases to exhibit a relatively even OD response over the 70 to 125 kVp range. It is this type of image medium response characteristic that the AEC must compensate for to maintain consistent image quality over the clinical kVp range.

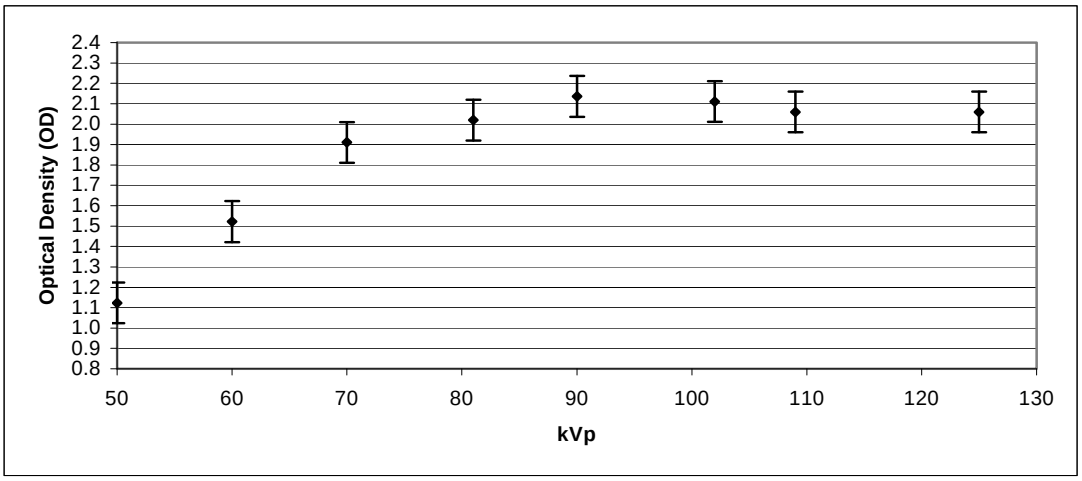

Figure 3.2 Typical kVp response of a Kodak T-Mat-G-RA type screen-film system to a fixed dose of 0.8 mR

3.3 Radiographic film processing

Following an x-ray exposure, the screen-film cassette is opened in a dark-room where all normal light is excluded and only a light source to which the film is insensitive is provided to enable personnel to work. The radiographic film is removed from the cassette and placed into the entry rollers of the automatic film processor to begin the image development process.

Radiographic film, like any emulsion film based on some substrate, must be placed in chemical reagent baths which act on the chemicals of the film emulsion to develop the latent image trapped within its chemical structure. Gelatine and silver halide are the two most important components of the film chemical structure. The gelatine provides a suspension medium for the silver halide and forms an emulsion layer on the substrate of the film. When the silver halide is exposed to light from the fluorescing screen its chemical structure changes to form latent image sites. These sites are clumps of silver atoms that collectively represent the image. The film development stage locks this image onto the film substrate and removes any other emulsion material that does not contribute to the image.

Radiographic film and processing chemicals must be carefully managed since images of consistent quality cannot be assured with expired film and chemicals. Bulk film should be stored in a dry, temperature-controlled area isolated from direct x-ray sources in light-tight containers to avoid fogging.

3.4 AEC setup for screen-film

The algorithm applied to an AEC control unit is designed to program the AEC to compensate for the kVp response irregularities of the image medium. When this is achieved, consistent image quality is assured over the clinical kVp range. The algorithm which provides this image consistency sets the AEC to control exposure time and therefore the dose applied to the image medium. The exposure is terminated when the detectors in the AEC control device have received the required dose.

3.4.1 AEC dose set-point

The AEC controlled dose for any exposure is based on a chosen target value on the linear section of the film's characteristic curve response. This target dose value is called the 'dose set-point'. The dose set-point is the set up reference dose for the AEC control over the clinical kVp range and should produce an image OD that is within the range 1.2 to 1.4 (NRL C5 1994). This avoids the shoulder and toe areas of a film characteristic curve which are non-linear and so give relatively poor contrast definition for large increases in dose. The 'dose set-point' is agreed upon through a consultative process between physicists, clinicians and equipment manufacturers. There is no universally accepted standard for this dose value and so it is based on a compromise of two opposing requirements. The first of these requires sufficient dose to the image medium to produce a satisfactory film OD, to maximise contrast variations in the

image. The second requirement is to minimise patient exposure dose and hence to prevent the possible onset of medical complications. Higher exposure levels are potentially harmful to patients and violate the legislated requirement to keep doses as low as reasonably achievable (the ALARA principle).

The exposure used to determine the AEC dose set-point is specified by kVp, PEP thickness, SID and AEC chamber selection. The specified values for this exposure at Christchurch Hospital are 81 kVp, 150 mm Perspex PEP, an SID of 1000 mm and the selection of the central AEC chamber. The dose delivered to the plane of the screen film, in the Bucky tray, under this test exposure is measured and compared to the required dose set-up value. The AEC dose control is adjusted and the procedure repeated until the correct value is attained. The dose measured at the plane of the image medium under these circumstances is approximately 3.0 µGy. Having achieved the dose required a second exposure is performed and the OD value of the homogenous film image is measured from the image centre and recorded. This OD value becomes the target exposure index for the process of setting the AEC dose control to compensate for the kVp response of the image medium.

3.4.2 AEC setup to compensate for the kVp response of the image media

AEC devices are designed to automatically control x-ray exposures of different anatomical structures and patient size over the clinical kVp range. Under the control of the AEC the dose to the screen-film combination should be consistent and producing consistent image quality. In order to achieve this optimally, they must adjust the dose to compensate for variations in the kVp response characteristic of the imaging medium. The kVp response characteristic of the image medium can be determined by measuring the exposure dose at the plane of the image medium over the kVp range tested using a manual technique at a fixed dose. The film OD will vary according to the variations in kVp response characteristic of the image medium.

To set up the AEC the AEC dose control is adjusted for each kVp setting to achieve the target OD on each exposed film image. The AEC control voltage references, described in section 2.6, which control these doses, are then locked into the AEC control circuit memory. These doses are all based on the value at the AEC dose set-point.

Provision can be made in the design of an AEC for manual adjustment of the AEC dose-point when required to compensate for extremes of patient sizes. This is achieved on the Philips Optimus x-ray machine used for this thesis by varying the density control setting. When this is done the AEC control algorithm maintains its normal control function over the kVp response of the image medium but the dose set-point it is normally based on is increased or decreased as required. The density control function is typically enabled by a manually operated switch function.

3.4.3 AEC test procedure with screen-film

To ensure the stability and accuracy of the calibration of any AEC device, quality control tests are required to be carried out by medical physicists on a regular basis, typically annually (IPEM report 91).

The standard range of physics tests for AECs listed in section 3.1 is performed by the Medical Physicist. All tests are performed at the SID for which the Bucky and its associated grid have been designed. The SID is typically 100 cm for table Buckys and 140 cm for erect Buckys. The AEC test procedure applied by the Medical Physics group at Christchurch Hospital utilises 75 mm thick Polymethyl Methacrylate (Perspex) slabs for its patient equivalent phantom (PEP) simulation material. For the full range of tests, up to four of these Perspex slabs are used to simulate a reasonable range of patient size. The PEPs are placed in front of the Bucky assembly and positioned to cover all three AEC chambers. The x-ray beam is collimated to form a 300 mm × 300 mm field size at the Bucky. The film cassettes, loaded with film, are placed in the cassette tray of the Bucky assembly. A film image is required for each part of each test function, resulting in the production of twenty eight or more individual films.

The ODs from the test images are measured and recorded for all test exposure conditions. These recorded values should lie within the range of acceptable OD values 1.2 - 1.6 (NRL C5 1994).

3.5 The perspex patient equivalent phantom

Verification of AEC performance is best carried out under clinically relevant conditions (Goldman and Yester 2004). Due to its composition perspex used as the PEP material effectively simulates the characteristics of the human body. Radiographically the human body is very similar to water, being approximately 98%

water by composition. Perspex is also radiographically similar to water as shown in Table 3.1 and therefore to the human body.

In table 3.1 *Z* is the average atomic number of the material, *A* is the average mass number and *I* is the mean excitation energy per ion pair. The perspex PEP is simpler and safer to use around mechanical and electrical equipment compared to the more traditional water phantoms. However, there are weight and size considerations with its handling and transportation. Each PEP weighs approximately 8.5 kg and has dimensions of 370 mm × 320 mm × 75 mm. The longer dimension has been machined to form a 50 mm carrying handle. The Perspex slabs are physically stable, radiographically uniform and offer good positional accuracy relative to the AEC chambers associated with x-ray machines. These attributes of perspex were important in the decision to use the perspex slabs as the PEP material for the experimental work required for this thesis.

NOTE:
This table is included on page 31 of the print copy of the thesis held in the University of Adelaide Library.

Table 3.1 Radiographic comparison: PEP to human tissue. (Data reproduced from National Institute of Standards and Technology (NIST) x-ray mass attenuation tables)

3.6 The lead window device for testing AECs

The handling and processing of all the cassettes and films required to fully test an AEC, is a significant factor in the time required to perform AEC functionality testing. The following describes a device which greatly improves the efficiency of the testing technique by reducing the number of films required to determine the performance of an AEC.

The lead window test method is described in a paper by Hunt and Plain (1993). In the version of this method used at Christchurch Hospital, a single 35 mm × 35 mm film cassette has been modified to mount a 2 mm thick lead sheet over its whole surface with a 200 mm diameter hole cut out of the centre. This hole is filled with a 2 mm thick lead disc which has a diameter slightly less than the hole in the lead plate so it is free to rotate within the lead plate. The lead disc has a single cut-out sector as shown in Figure 3.3. This diagram shows the sector window ready for exposure 1. The lead disc is rotated one step for each separate test exposure, to open a window to a new sector of the film contained within the cassette. The 2 mm thickness of lead protects

the other parts of the film from radiation. The size of the lead disc cut-out is designed to provide sufficient sectors to enable as many images as required to complete a section of the AEC test sequence. The only physical constraint on the number of sectors in the disks circumference is the need to ensure a reasonable sample area to measure the OD of the film image and also to minimise any radiation or scatter from adjacent exposures. The rotating lead disc used at Christchurch Hospital provides for 18 separate exposures. In order to perform the full range of AEC tests, 28 exposures are performed which can be accommodated on two films. If individual films are used for each test then 28 films would be required as stated in section 3.4.3.

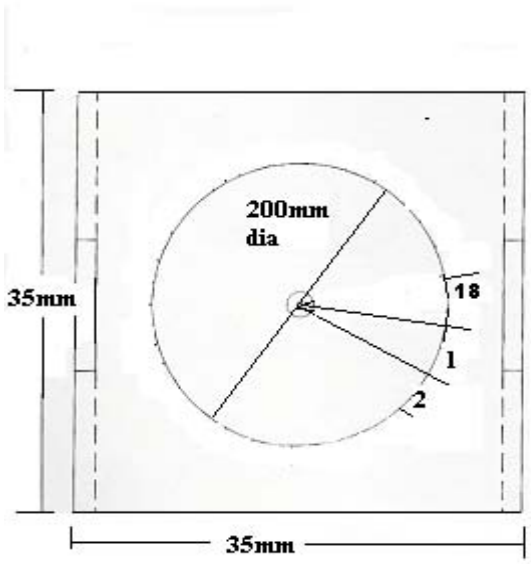

Figure 3.3 Physical layout of the AEC test cassette showing film window at position 1

The use of the lead window method is limited only by the physical size of the test cassette. The test cassette with its lead disc assembly must be physically thin enough to fit inside the limited space available within the Bucky assembly used for normal screen-film cassettes. The depth of this space is approximately 20 mm for a standard Philips Optimus x-ray machine Bucky but this may vary for machines of different manufacture. The depth of the test cassette used at the hospital is 18 mm. This compares to a depth of 15 mm for a standard x-ray screen-film cassette

3.7 AEC test results

The assessment result for each AEC test function is determined by first calculating the average OD of the images within each test assessment area, for example kVp or PEP thickness. The average density should be 1.2 and the range should be within 1.1 - 1.3.

Average OD values lower than the standard OD range result in images which are lighter and lack sufficient contrast for good image diagnosis. Higher OD values indicate a darker image where fine or lower contrast image detail may be lost and also indicates higher clinical x-ray doses. The maximum OD variation of the individual results from the average within each separate assessment area is also calculated. For repeatability tests using the same exposure conditions this variation limit is $\leq$ 10% while the limit for variable exposure conditions is $\leq$ 20%. If the result exceeds the test limit, the AEC is recorded as having failed the particular function.

The AEC dose set-point is checked with a measurement of the dose from the centre chamber test as described in section 3.4.1.

The complete set of AEC results and their assessment is documented and becomes part of a report produced by the Medical Physicist which details the complete operational status of the x-ray machine. It is the responsibility of the equipment maintenance engineers to correct any non-conformance of the machine's performance, including AEC functionality.

Chapter 4

The Digital Environment with Computed Radiography

4.1 Introduction to digital imaging

The development of digital imaging systems which includes computed radiography (CR) has brought about a steady decline in the use of radiographic film systems as the primary mode of x-ray imaging. Consequently, a review of all physics test procedures including AEC functionality test procedures is required to assure their compatibility with the imaging characteristics of digital imaging systems (Huda 1997).

There are many digital imaging media available on the market including complementary metal oxide silicon (CMOS) devices, charge coupled devices (CCDs) and thin film transistor (TFT) detector arrays. The calibration procedures described in this thesis in relation to CR can be adapted to any of these systems. At the time of writing this thesis, NRL had no published documentation or guidelines on the requirements for AEC functionality testing in any digital imaging environment.

4.2 CR technology

CR technology has developed since its conception to become one of the most common digital imaging modalities in radiology departments today. It became commercially available in 1983 with the introduction of the Fuji FCR101 system (Bradford et al 1999). CR technology is adaptable to digital radiography that enables the application of advanced image enhancement techniques (Crawford and Brixner 1991). "The broad acceptance of CR has been due to its large dynamic range, digital nature, easy portability and uniqueness rather than its intrinsic image quality" (Rowlands 2002).

CR technology is based on the detection of x-rays by photostimulable phosphors (PSPs). PSPs are one of the most successful modes of x-ray radiation detectors (Yaffe and Rowlands 1997). The PSP stores absorbed x-ray energy in crystal structures and is sometimes referred to as a 'storage phosphor' (AAPM Task Group 10 2002). The best phosphors have efficiencies for x-ray radiation absorption of between 10 and 20% (Rowlands 2002).

Kodak CR PSPs are formed onto a rigid substrate called an image plate (IP) which is contained in a protective cassette similar to a conventional screen-film cassette. They are compatible with conventional x-ray machines, enabling hospital x-ray departments to convert to a CR system without the need to invest in dedicated digital x-ray machines. Most installations closely emulate radiographic film radiography with the use of cassette based image systems. Although CR image plates are initially expensive, they can be reused for thousands of exposures.

The CR cassette is a light tight enclosure for the IP. The purpose of the light-tightness of the cassette is entirely different to that for screen-film systems. An x-ray film is sensitive to normal room lighting and will be completely fogged (darkened) by exposure to this light. Conversely, exposure of a CR PSP to the same light will cause any latent image on the PSP, produced by exposure to x-rays, to be erased.

4.3 The PSP response to x-rays

As discussed in section 3.2, x-ray photons incident on a screen-film cassette interact in a luminescent screen which emits light that permanently modifies the chemical structure of the associated radiographic film, to form a latent image. When the imaging medium is a CR PSP, the x-ray photon directly excites the electrons in the atomic structure of the phosphor material. The PSP is an energy integrating device where the energy deposited on the PSP depends on the absorption characteristics of the phosphor material and the energy spectrum of the incident x-ray. A latent image is formed from this energy deposition. To read this image, the PSP is scanned by a laser contained within a CR processor which de-energises the excited electrons. This change in the energy state of these electrons releases energy in the form of light in a process called photoluminescence which is described below. This emitted light, contains the image information and is collected by a photomultiplier tube. The PSP is restored to its original state by the application of strong white light. This process restores any remaining excited electrons to their pre-excitation state which erases any latent image remaining on the PSP. The PSP is then able to be used immediately for another exposure.

4.3.1 The Mechanism of Photoluminescence

Rowlands has described in his topical review titled ‘The physics of computed radiography’(2002) the process by which x-ray radiation incident on the phosphor of a CR IP produces latent image sites consisting of trapped charges within the phosphor.

The sites containing trapped charges have strong optical absorption bands especially in the 633 nm (red) band, which is the wavelength of He-Ne gas lasers commonly used to scan the image in a CR reader as described in section 4.8. The particular CR PSP referred to in this work is the barium fluoro halide, $BaFBr_{0.85}I_{0.15}$: $Eu2^+$ using bromine as the halide. This phosphor is now the most commonly used by many CR PSP manufacturers. In comparison to the simpler form BaFBr I: $Eu2^+$ used in earlier versions, this new phosphor has a marginal increase in x-ray absorption and has a better spectral match to the wavelength of maximum phosphor stimulation with solid-state diode lasers. Solid state lasers have a spectral wavelength of 680 nm.

The mechanism of the photostimulable luminescence has been reported as being not completely understood with at least two models being proposed, one being monomolecular and the other bimolecular (Bogucki et al 1995). A band model using the bimolecular approach offers a possible explanation for the process.

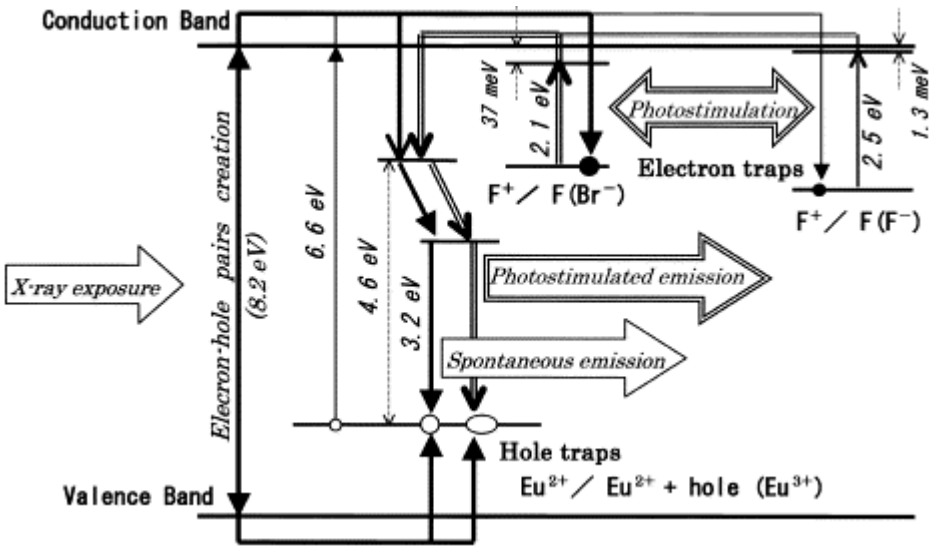

Figure 4.1 Energy level diagram of PSP (Reproduced courtesy of Kenji Takahashi with permission from Elsevier Limited)

This model shown in Figure 4.1 should be viewed with the following explanation quoted from Takahashi (2002): "When exposed to ionizing radiation, a number of electron–hole pairs are generated, proportional to the radiation energy absorbed by the phosphor particles. They immediately recombine to either emit light from the excited states of the Eu^{2+} ions or create quasi-stable F-centres. An F-centre consists of an electron trapped by the F^+-centre. An F^+-centre is a halogen ion vacancy created by controlling the formation process of the phosphor. These F-centres and corresponding

hole traps store the energy of the absorbed ionizing radiation. When exposed to red laser light, used for reading the IP, energy is absorbed by the F-centres and the trapped electrons are raised to excited states where they are thermally excited to the conduction band. They recombine with holes trapped by Eu^{2+} ions, which forces the excited Eu^{2+} ions to emit light corresponding to the 5d–4f transitions."

The quasi-stable 'F' (Farbzentren) centres are a characteristic of halide crystals subjected to x-ray radiation. These centres are anion (negatively charged ion) vacancies occupied by electrons (Seggern 1999). The electron – hole recombination process that emits light is known as photostimulated emission. The spontaneous luminescence and photostimulated luminescence emitted by the phosphor both have similar optical spectra in the 390 nm (blue) wavelength range.

4.4 PSP sensitivity to low energy radiation

Barium which has a lower K-edge at 37.4 keV than its screen-film counterpart, gadolinium at 50.0 keV, is the main absorption agent in the CR phosphor material. There is controversy in the relevant literature as to whether the increase in scatter to primary ratio response in CR is due to this lower K-edge or to the relatively poor absorption of CR phosphors (Seggern 1999).

The absorption K-edge of a material is the applied energy required to eject an electron from the first or 'K' shell of an atom. When this energy is applied, electrons in this shell are released; de-excitation of the excited atom results in the emission of characteristic radiation. In section 2.5, Figure 2.4 shows an example of how this characteristic radiation appears on the radiographic spectrum for tungsten which has two main characteristic radiation peaks. The most energetic of these occurs at about 69.0 keV from interactions involving electrons in the higher energy 'K' shell of tungsten's atomic structure.

Figure 4.2 shows the x-ray absorption response for gadolinium oxysulphide (Gd_2O_2S), a luminescent screen used for screen-film systems and a PSP ($BaFBr_{0.85}I_{015}$: Eu^{2+}). The relative intensity of the primary x-ray beam is also displayed in this graph to provide a perspective on the relevance of the absorption response at each energy measured. The data for this graph were collated from two sources. Firstly, the x-ray spectrum data were obtained from NRL's 'Specgen' computer program developed by Glen Stirling and based on the Birch and Marshall model. Secondly the absorption spectrum for the luminescent screen and PSP

phosphor was obtained from the International Atomic Energy Agency (IAEA) computer program 'xmudat' version 1.0.1 (Nowotny 1998).

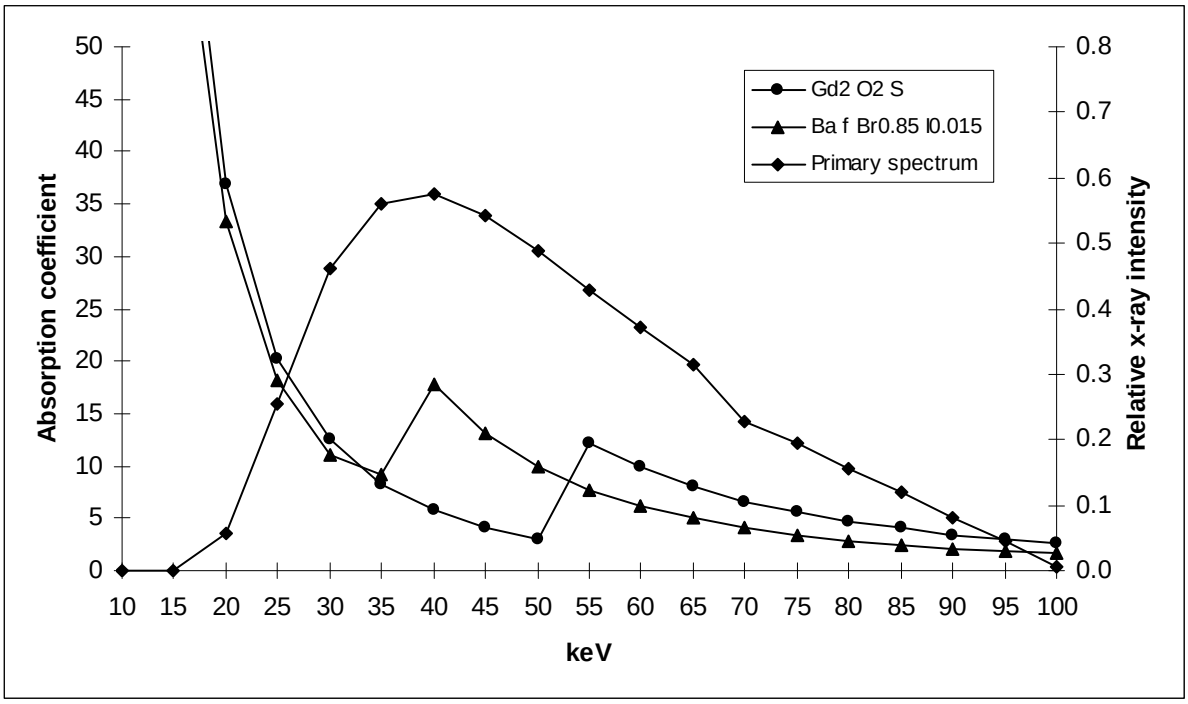

Figure 4.2 X-ray absorption vs photon energy

The 'K' edge for the luminescent screen appears around 50 keV, characteristic of the main absorbing medium gadolinium. The main absorbing material in the PSP is barium which has a 'K' edge around 37.4 keV. The absorption characteristic between 35 keV and 50 keV is greater for the PSP, which supports one of the theories for the increased sensitivity of CR to scatter radiation. However analysis of the absorption characteristic over the whole range of the primary x-ray beam spectrum (10 – 100 keV) by calculating the area under the absorption characteristic for each material produces similar results. This does not support the general theory that a PSP has a poorer overall absorption characteristic although comparisons at individual keV points not included in the 35 keV to 50 keV range do exhibit slightly poorer results.

In conclusion, we can see that the response characteristics for these two phosphor materials are almost identical except for the 35 keV to 50 keV range where the PSP exhibits a higher sensitivity. Any scatter radiation within this keV range will be preferentially absorbed by the PSP compared to the luminescent screen. This scatter increases the noise (signal content not directly related to the imaged object) content of

a CR image and reduces the SNR. The noise sources contributing to noise in CR images are discussed in section 4.8.

Scattered radiation emitted from a patient or PEP placed in the x-ray beam will be of lower energy than the primary x-ray beam. A phosphor material that discriminates between this lower energy radiation and that of the primary beam can, partially at least, filter out this unwanted and confounding contributor to the resulting x-ray image (Bogucki et al 1995). The gadolinium based luminescent screen has this ability for scatter energies within the range 35 keV to 50 keV.

During the earlier development of CR the observed sensitivity of a PSP to lower energy x-rays prompted the belief that doses to patients could be reduced below the doses used for screen-film systems. However it was soon apparent that the noise content of CR images at these lower dose levels made image diagnosis difficult. Consequently patient x-ray exposure doses using CR as the imaging medium have generally been increased although there is currently no standard for this (Bushberg 2002).

4.5 Image exposure index

When a clinical CR image has been processed the resulting image is presented on a viewing monitor which allows the radiographer to confirm the placement and positioning of the anatomy required. This image also displays an indication of the exposure level in the form of an EI value which can provide an indication of the quality of the x-ray. The EI value attributed to an image is a unit-less integer value of the average pixel value, described in section 4.8, over the whole clinically useful image. The image EI value is also used by medical physicists to evaluate the calibration of a CR machine and to assess the functionality of an AEC device associated with CR. The images used for this purpose are produced by exposing a CR cassette to a uniform x-ray beam over the whole IP surface area to produce a homogenous image from which an accurate EI value can be recorded. The relationship between x-ray dose applied to an IP and the EI for a Kodak CR system using GP-25 screens quoted by Kodak is given by the following equation:

$$EI = 1000\ (\text{Log}\ (\text{x-ray dose in mR})) + 2000$$

The exposure index indicator for the image processing system should match the dose value applied to the image medium according to its designed algorithm. A regular

program of CR equipment maintenance is required to ensure a consistent exposure index indication for the same applied x-ray dose to the imaging medium. The medical physicist confirms these values for a range of applied doses. At Christchurch Hospital these tests are carried out in air and are not as susceptible to the level of scattered radiation present when measurements are performed within the confines of an x-ray Bucky tray as used in the experimentation for this thesis.

4.6 CR response as a function of kVp

With any x-ray imaging medium, the response to varying kVp is a characteristic of the atomic configuration of the medium. To determine this characteristic a series of tests were conducted over the clinical kVp range to record the EI values of the images produced. The CR response tests must be conducted at a fixed exposure dose.

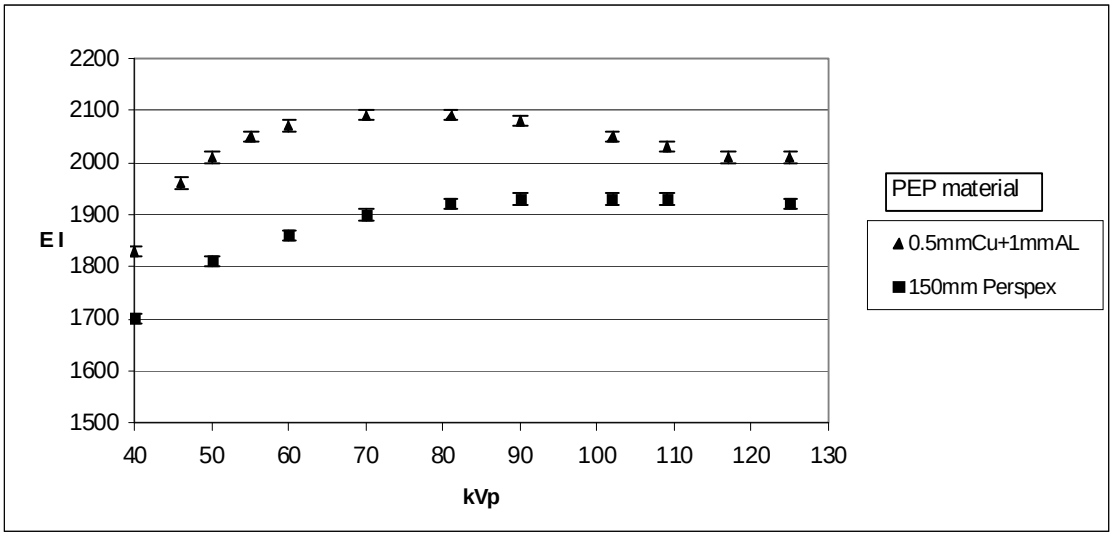

Figure 4.3 The kVp response of a Kodak CR PSP exposed to 1.0 mR

Figure 4.3 shows the results of tests performed experimentally on a Philips x-ray machine using a fixed dose of 1.0 mR. A Kodak CR reader was used to process the test images. The error bars indicate a possible range of ± 10 exposure index values. This error has been determined from experimental data and is based on the readout resolution of the Kodak reader as explained in section 4.12. The experiment compared the results for two PEP materials, 0.1 mm Cu with 1 mm Al and 150 mm Perspex. The response obtained is typical of those found in many reports and papers for Kodak CR phosphors and shows significant variation in EI with kVp, especially for the Cu and Al PEP (Lu et al, 2002). The kVp response of an image medium is required to provide the data which enables the AEC of an x-ray machine to be calibrated optimally to provide consistent exposures over the clinical kVp range.

4.7 The CR response as a function of dose

Current CR readers use photomultiplier tubes (PMTs) to detect the stimulated light output from CR PSPs and these achieve reasonable linearity over four orders of exposure magnitude. An experiment was conducted to derive the exposure range response for a Kodak CR system at Christchurch Hospital. In order to obtain the required data for this, two x-ray exposures were required at each dose setting. The first was used to measure the exposure dose that would be received by a cassette in the Bucky tray. This was achieved by placing a 15 cc ion chamber in the centre of the Bucky tray in the same plane as a CR cassette. The second exposure was required to expose a CR IP and obtain the EI data from the processed image. The x-ray machine was set to perform these exposures at 81 kVp which enabled a comparison with published responses. The dose values required to show the complete range of the response of a CR PSP were achieved using a range of SID, tube current and exposure time combinations.

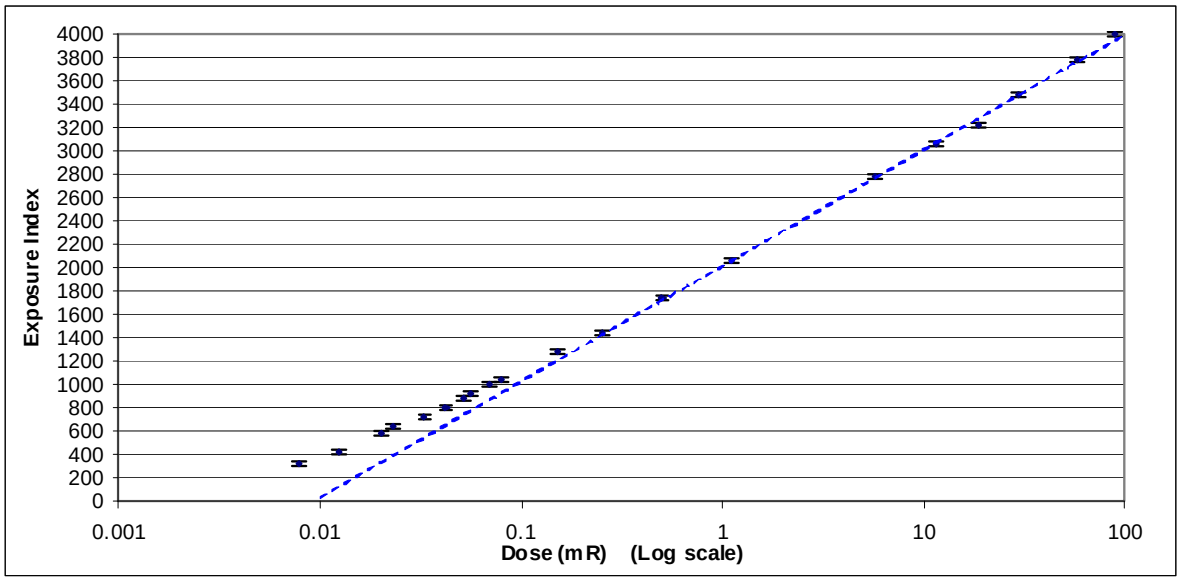

Figure 4.4 The exposure dose range of a Kodak CR system

The range of possible EI values for a Kodak CR system is 0 to 4096. The response obtained from the acquired data is shown in Figure 4.4. The results compare well with typical exposure range responses of CR PSPs given in many reports and papers such as the AAPM Task Group 10 report and the paper by Wilkinson and Heggie (1996). The dashed blue line on the graph represents the Kodak dose / EI relationship given in

section 4.5 for GP-25 PSPs. Within experimental error the test results for doses above 0.25 mR conform well to the Kodak formula. The gradual deviation away from the ideal Kodak formula line of the experimental results below 0.25 mR is a result of the decreasing signal to noise relationship of the PSP. This effect is also exacerbated by the offset factors for variation to laser power output which is added to image data. This leads to the situation where an erased PSP is unlikely to produce a zero EI value and can be up to 100 EI values (Bogucki et al 1995).

Used in conjunction with the digital image enhancement available on CR workstations, a wide range of exposure results can be accommodated to produce an acceptable image. This ability is a distinct advantage over screen-film systems where the film image produced is fixed. However the wide dynamic range of CR must be treated with caution to avoid patient over exposure and to avoid the risk of reducing exposures to such a level that noise masks clinically sensitive image information. The exposure flexibility allowed by this dynamic range can be used to great advantage. However the potential to mask inappropriate radiographic techniques should not be overlooked. For this reason, it is prudent for radiology departments to put in place an auditing process that monitors exposure dose and image quality.

4.8 Image processing with the Kodak CR reader

The CR reader performs a similar processing function for PSPs as a film processor does for radiographic film. The latent images formed in both mediums by exposure to x-ray radiation are acted upon by their respective processor functions to produce a visible image of the target subject.

Each CR manufacturer employs their own unique method of processing their PSPs. The IP contained within the Kodak CR cassette has a unique identifying bar code. The MRT moves this bar code in front of the bar code reader attached to a remote operators panel (ROP) to register the cassette for a particular examination. The ROP is a computer workstation and is generally located near the x-ray room it serves, with a communications link to the CR reader. The bar-code data is automatically inserted into the appropriate area of the patient demographic data form on the ROP screen. The ROP serves as an image viewing station where the MRT can verify image quality and perform digital image enhancements. It is also the interface by which the patient's demographic data and hospital patient recording data is input and linked to the particular CR cassette used for a patient's examination.

Once the patient's demographic data has been input to the ROP panel the MRT is able to select pre-processing options which provide exam specific optimisation. It achieves this optimisation by adjusting the processing sensitivity at certain points on the image pixel histogram. The cassette is then placed into the CR reader. The machine opens the cassette in a light sealed cavity and the IP is extracted. The PSP is scanned by a He-Ne (633 nm) or diode laser beam which begins the process of photostimulated luminescence (PSL) (Rowlands 2002). The sampling aperture is the instantaneous area of the phosphor screen stimulated by the laser beam. The ratio of the sampling rate and the scan rate across the PSP determines the size of the sampled area known as a pixel. Also the speed of the PSP movement in the sub-scan (vertical) direction is coordinated with the horizontal movement across the PSP such that the pixel length is equal to its width. The pixels are square. The pixel dimension in the scan direction is typically between 100 µm and 200 µm dependant on PSP size. As the laser beam passes over an area of the phosphor it releases charges trapped by the reaction to incident x-rays and this stimulates the emission of light from the phosphor. The light emitted is guided to a photomultiplier tube (PMT) within the reader. The PMT detects this light and converts it to an electrical signal proportional to the amount of light produced. This analogue signal is then digitised to form the raw data that represents the imaged object. This is achieved by quantising the average signal amplitude at the individual pixel location. The quantising of the analogue signal pixels into discrete integer values is determined by the amplitude of the signal present in each sample and the total number of possible discrete values. Kodak has 4096 possible discrete values. A pixel clock coordinates the time at which a particular signal is digitally encoded to a physical location on the scan line (AAPM Task Group 10 2002). This timing is determined by the pixel dimension in the horizontal laser scan direction and the total number of pixels in that direction relative to the CR cassette size. The discrete signal amplitude at each pixel location and the timing of their measurement ultimately define the system resolution (Bogucki et al 1995).

Table 4.1 Kodak screen and pixel sizes (Bogucki et al 1995)

Kodak PSPs are manufactured to several different physical sizes. Each has a unique image size measured by the number of pixels in each orientation as shown in Table 4.1.

Kodak initially quantises the PMT signal range to 2^{16} (65536) bits or gray levels in order to implement a digital logarithmic transformation to the final 2^{12} (4096) bit image data. Pixel sampling data is derived from the 16 bit raw image data output from an analogue to digital converter. The raw 16 bit linear image data is mapped to 12 bit logarithmic data to enable correct weighting of the digitisation across the four decades of radiographic exposure to which the PSP is able to respond (Bogucki et al 1995). This dynamic range compression preserves digitisation accuracy over a limited number of discrete gray levels. Logarithmic conversion also provides a linear relationship of incident exposure to output signal amplitude (Seibert 2004). The transformation to 2^{12} bits provides weighting of the digital signal for better visualisation on a monitor (Rowlands 2002).

The 2^{12} bit digital stream representing the exposed image is the data that is stored in the PACS image storage system and which is later retrieved and viewed on workstations at the request of radiologists or clinicians for image analysis and diagnostic reporting.

A 2^{8} bit digital stream is derived from the 2^{12} bit data and used to generate the image produced on the ROP that the MRT uses for image verification following an examination. The image data from the CR reader used for image presentation and storage is formatted to the Digital Imaging and Communications in Medicine (DICOM) standard described in section 4.8.1.

Once an IP has been scanned by the laser it is exposed to white light to erase any remaining image latency. Modern CR readers can process a PSP, including erasure time, in less than one minute. The IP is returned to the cassette and then expelled from the machine.

The Kodak 900 CR readers in place at Christchurch Hospital have a processing throughput of more than 60 plates per hour. The later Kodak CR950 systems can process up to 86 plates per hour. The time required to process a CR IP is an important component in the workflow of a busy radiology department.

4.8.1 The DICOM standard data interface

A digital interface provides the communications link between the Kodak CR reader, ROP and the PACS database and archive. The interface specifies the format of the image and data information. The American College of Radiology (ACR) and National Electrical Manufacturers Association (NEMA) formed a joint committee to develop a

standard for digital imaging and communications in medicine. The digital image DICOM Standard evolved from this and was developed according to the NEMA Procedures and patterned after the Open System Interconnection (OSI) of the International Standards Organisation (ISO) (NEMA 2003).

DICOM 3.0 is the current version of this standard and Part 14 of this describes the grayscale Standard Display Function (GSDF) used in the display of the digitised CR images. It specifies a function that relates pixel values to displayed luminance levels on the viewing monitors. Other parts of this DICOM Standard specify how digital image data can be moved from system to system and how these images should be displayed.

4.9 Working with the processed image

The image processed by the Kodak CR reader is displayed on an ROP so that the MRT can assess image quality including anatomical content and positioning before image archiving to a picture archiving and communication system (PACS). The digital nature of CR imaging systems enables image manipulation with digital transformations. The MRT is able to apply local post-processing techniques to further enhance the presented image. Post processing options such as noise suppression, grid line removal and edge enhancement is performed, if required, on the image data before its delivery to the image storage system (AAPM Task group 10 2002).

The ROP image presentation available to the MRT is designed for local assessment of image quality and positioning only. It is not designed to perform to a diagnostic image standard.

4.9.1 CR PSP erasure process

An important part of the regular maintenance and physics checks of this equipment is to ensure that the erasure process is functioning within set limits of acceptance. Incomplete PSP erasure can result in image artefacts on subsequent images.

Once a PSP is read by the CR processor the remaining latent image is erased. A bank of high intensity fluorescent tubes within the CR processor performs this task and ensures that the process of erasure is thorough and completed within a short time interval. The total CR IP processing time for a CR 900 reader is approximately 1 minute. The IP erasure process occupies approximately 20 s of this total time. The erasure process is required to remove all image information. In practice natural

radioactivity and cosmic radiation can accumulate on IP's such that there will always be some residual activation within the PSP.

4.9.2 Image storage and retrieval: PACS

Digitally encoded radiographic images from digital imaging systems are stored in large capacity (multiple terabyte) memory systems. This memory must be accessible on demand to retrieve and display patient images within a few minutes of any request. A PACS is designed to simplify image retrieval, enable multiple viewing of images and provide the security of a large density digital image storage system with backup facilities. From the time the image has been stored into a PACS it is then immediately available throughout the internal hospital network or via external networks (telemedicine). On request these images can be viewed at appropriate high-resolution workstations for diagnostic analysis by radiologists. A single image or multiple images can be requested and retrieved simultaneously at multiple workstation locations allowing conference style image analysis and diagnosis confirmation. These workstations use imaging software packages to apply advanced digital enhancement techniques to manipulate images and maximise their visualisation. The benefits of these digital processing and image storage systems make them a very attractive option for hospital radiology departments.

4.10 Noise characteristics of CR imaging

Noise in a radiographic image is variation in the signal not caused by subject anatomy. There is a wider range of noise sources contributing to image distortion for any digital system than for film based systems. These can be classified as follows.

Quantum noise (quantum mottle) is the dominant noise factor on under exposed images. Quantum mottle occurs in both screen-film and CR systems, and is caused by the non-uniformity of x-ray photons absorbed per unit area of the screen. It is based on Poisson statistics where the standard deviation is $\sqrt{N}$ where N is the average number of x-ray quanta per unit area. Quantum noise varies as the square root of the number of x-rays used to produce the image. As the x-ray exposure increases, the fractional contribution of this noise decreases (Wilkinson and Heggie 1997). Increasing the phosphor thickness reduces quantum mottle by increasing x-ray absorption but spatial resolution will be adversely affected.

Conversion noise is the variation in signal detected per absorbed x-ray and is inversely proportional to x-ray exposure. The conversion efficiency value for a

particular phosphor is determined by its composition and design. A high conversion efficiency increases screen sensitivity and reduces patient exposure. Unfortunately, an increase in conversion efficiency decreases the quantity of x-rays that must be absorbed in the phosphor, and this increases quantum noise. The only way to increase phosphor sensitivity without increasing quantum noise is to increase the absorption efficiency. An increase in absorption efficiency does not change the amount of radiation that must be absorbed to produce an image. The design of the phosphor is therefore based on a balance between screen sensitivity and quantum noise.

Photon or luminescence noise is the inherent statistical variation in the detected photons that are stimulated out of the phosphor screen and is inversely proportional to the x-ray exposure. Ideally a phosphor should emit the same amount of light from the absorption of every x-ray. However in practice the light output from the phosphor varies and this inconsistency contributes to image noise. The noise is produced by the variation in the intensity of the emitted luminescence and the phosphor penetration depth of the stimulating laser beam.

Structure noise is the spatial gain variation in the screen (granularity) and is independent of the x-ray exposure. This noise is proportional to the amplitude of the derived image signal and is more apparent at very high x-ray exposures. It is reduced at higher spatial frequencies due to pixel signal averaging caused by the laser light spread to adjacent pixels Structure noise is relatively insignificant in most radiographic applications.

Laser noise is due to the fluctuation in the output intensity of the stimulating laser and is independent of x-ray exposure. This type of noise produces low frequency components within the noise spectrum. The CR processor minimises this noise by detecting the intensity fluctuations of the laser output and adjusting the image signal accordingly.

Electronic noise is independent of x-ray exposure. It is due to signal amplification and conditioning and is a very small contributor to the overall noise. This noise contributor can be minimised by the use of high quality, low noise components in the manufacture of the electronic circuitry processing image signal information within the CR processor.

Quantisation noise is independent of x-ray exposure and is due to the conversion of the continuous signal output from the CR reader’s photomultiplier into discrete values

by the digitisation process and can be minimised using an adequate bit depth system i.e. range of quantisation steps.

All of the above noise components have a spatial frequency dependence such that lower spatial frequencies contribute more to the overall noise power spectrum especially at low exposure levels (Yaffe and Rowlands 1997).

CR is considered to be a noise limited system such that the SNR is largely determined by the x-ray dose applied to the PSP, especially at extremely low doses. The SNR at very low doses is poor, due to the base noise contributors such as Structure Noise and Laser Noise, which are independent of the x-ray exposure. When the effects of noise contributors such as quantum mottle become more apparent then the visualisation of a clinical image can be compromised. Higher exposure levels produce clear crisp images with good contrast that appear to have a better signal to noise ratio. However, saturated areas due to excessive exposure levels may mask anatomical features.

4.12 Processing time delay effects on exposed IP

The latent image formed from the x-ray energy deposited onto the PSP is stored in its crystal structure but fades exponentially over time. This fading is caused by the spontaneous phosphorescence processes occurring within the phosphor material.

A local experiment was conducted to derive the image decay characteristic of Kodak CR PSPs using a Kodak CR 900 processor. The results have been plotted in Figure 4.5. This graph shows that the EI decreases exponentially with increasing processing time delay. Following an eight hour processing delay the exposure index value has decreased by almost 10% compared to the value obtained when the image was processed immediately. This EI value recorded at this time delay was approximately 2730 which is approximately 300 EI values less than the value obtained at the 60 s delay interval. Using the Kodak dose/EI formula an EI variation of 300 points is equivalent to a delivered dose value equal to half of the original exposure. It can also be shown that a clinical image can be read out from an exposed IP even after several days of processing delay.

Delays in processing a PSP following its exposure to x-rays have an impact on the reported exposure index and on image quality. This factor is critical in obtaining accurate results for all standard Medical Physics testing procedures and for the assessment of AEC performance for this thesis. Kodak recommends a 15 minute

processing delay for physics testing procedures. After a 15 minute processing delay a point in the image decay characteristic is reached where the rate of EI change with time begins to decrease. The rate of EI change in the first five minutes of the image decay curve is shown as approximately 8 EI/min. The decay rate between 15 minutes and 20 minutes is approximately 2 EI/min.

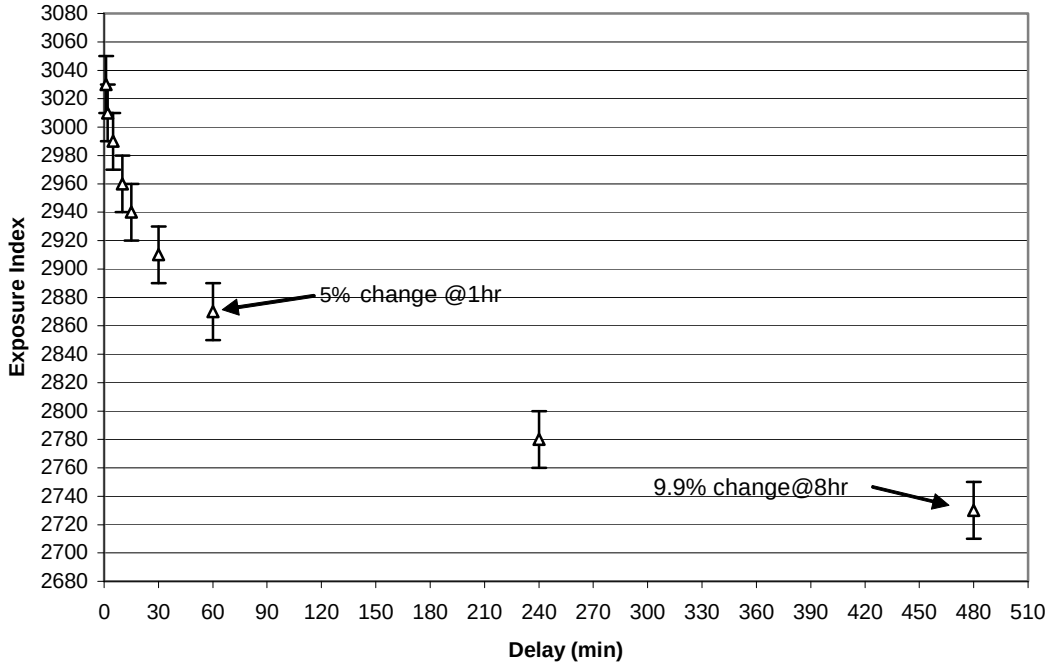

Figure 4.5 The IP response to image processing delay following exposure to 10 mR

Due to the large number of test exposures and the machine time required to complete this work, it was impracticable to conform to the recommended 15 minute processing delay. EI Measurement accuracy depends on consistent processing timing. The processing time is less critical at the 15 minute point on the processing delay curve but its accuracy is still dependant on test consistency. The practical alternative was to choose a much shorter delay and this was set for this thesis to be 60 ± 10s. This follows a similar process to that used by Doyle and Martin (2006) for their AEC calibration method (Doyle and Martin 2006). A Kodak CR 900 reader requires approximately 60 ± 10 s to processes a CR IP, resulting in a 120 ± 20 s time interval between exposure and EI readout. Typically, clinical images are processed immediately following x-ray exposure to obtain the required patient anatomical information as soon as possible and to determine if further imaging is required prior to

releasing the patient. Clinical images are therefore relatively unaffected by the processing delay effects presented above.

The first point on the image decay curve in Figure 4.5 shows the EI result of a CR image placed in the processor 60 s after exposure to x-rays. After the 60 s processing delay and the 60 s process time itself have elapsed the EI value has decreased by approximately 20 index points. It follows that the possible range of EI value inaccuracy for images processed with a 60 ± 10 s processing delay is ± 20 index points. The Kodak CR reader has a reporting resolution of 10 index points which implies that the actual EI variation lies within the range 15.1 to 24.9. This error represents a dose variation of 0.010 mR which is less than 2 % of the average dose measured for each scenario of the AEC kVp compensation tests.

In medical physics quality assurance and research environments, image processing delays can be a significant factor in output signal variance leading to inconsistencies of recorded exposure data. For this reason, a consistent processing delay is required.

4.13 Comparison of screen-film and CR

From a clinical perspective the requirement for CR imaging is to achieve comparable image quality to traditional film based systems.

CR was initially released as a package purporting to have several advantages over screen-film systems such as increased flexibility in image processing, improved reproducibility, a wider dynamic range, wider exposure latitude and reduced patient exposure (Bradford et al 1999). It is worth discussing these reported attributes in relation to image quality and control processes.

The ability to digitally enhance CR images is a major advantage over screen-film systems. This ability is made possible because image acquisition and display occur separately. An x-ray film image is a fixed physical entity which is unable to be altered at all. This means that if the processed image is unsatisfactory then the exposure must be repeated. CR images resulting from poor exposure techniques may be digitally enhanced to improve image visibility sufficiently to create a diagnostic image, thereby reducing the need for repeat exposures. However, the use of image processing software associated with CR may still be limited when extremes of exposures are encountered. AEC controlled exposures avoid the problems associated with under or over exposed images.

Early in the development of digital radiography, it was thought that its image quality should match the demanding resolution performance of screen-film based imaging. An alternate proposition is that a high value of limiting resolution is not as important as the ability to provide high quality image contrast over a wide range of x-ray exposures for all spatial frequencies up to the maximum possible limiting resolution (Yaffe and Rowlands 1997).

The spatial resolution of radiographic film is good because the film emulsion is usually no thicker than 10 μm (Heggie et al 2001). However its sensitivity to x-rays is poor due to the granular nature of the silver halide suspension in the emulsion. The low sensitivity of film was overcome when luminescent screens were introduced. In this situation the film is sandwiched between luminescent screens inside the cassette. The screens are more sensitive to x-rays than the film by itself and fluoresce to produce visible light to which the film is very sensitive. However the gain in sensitivity achieved by this is offset by a reduction in high spatial resolution due to light scattering processes within the phosphor of the screens (Seggern 1999). The negative effects of light scattering depend on the thickness of the screen's phosphor material. The problem is more significant on thicker screens but the inclusion of dye in the phosphor can help overcome this. The use of screens using rare-earth phosphors such as $BaSrSO_4$ with their increased absorption efficiency and conversion efficiency has become very important in screen-film radiology (Heggie et al 2001).

The response of a CR PSP to x-rays has limitations in spatial resolution due to the location of electron traps created within the PSP throughout the depth of the phosphor material. Scattering of the stimulating laser light increases image blur as it penetrates the phosphor and releases these traps over a wider area of the image than the size of the incident laser beam. Figure 4.6 illustrates the effect of the laser on a PSP and shows the scattering processes that occur. CR phosphor thicknesses vary between manufacturers. Kodak uses a phosphor thickness of 300 μm for their standard GP phosphors. The phosphor thickness determines the number of x-ray photons absorbed. Thicker phosphors increases light scattering and therefore reduces image resolution. While thinner phosphors produce sharper images, the amount of light released per incident x-ray photon is significantly reduced (Bogucki et al 1995). The effect of a thinner phosphor is similar to the statistical variation in the number of photons detected from the laser stimulation of the phosphor and results in image variation noise called photon or luminescent noise. Luminescent noise is described in section 4.10.

Film imaging has limited exposure latitude due to its characteristic curve response resulting in limited contrast resolution. A CR imaging system has a much larger exposure latitude.

NOTE:
This figure is included on page 52 of the print copy of the thesis held in the University of Adelaide Library.

Figure 4.6 The process of Photostimulated Luminescence (Reproduced with courtesy from J.Anthony Seibert, 2003)

A section relating to the cost analysis of a shift to CR imaging systems and image storage was originally included here but was not considered core to the project and therefore excluded. However should the reader wish to explore this subject area further I have included a reference to an introductory paper by Orand (2004) relating some of the issues of this cost analysis.

Chapter 5

AEC in a CR Environment

5.1 Introduction

Initially this thesis set out to explore the AEC testing protocol requirements when the imaging process is CR compared to the requirements for screen – film imaging systems. This exploratory stage determined that the only difference between the two protocol requirements for AEC was the methods used to extract image exposure information. The testing procedure requirements remain the same. However the most significant finding during this stage was not any differences in protocol requirements, but was an awareness that the AEC response over the clinical kVp range was not as consistent as expected. The function of an AEC is to maintain image consistency over the clinical kVp range. At this point the focus for the thesis was diverted towards the exploration of AEC performance and to realise any benefits from attaining a higher level of image consistency.

The AEC kVp compensation algorithm provided by Kodak for their CR systems and installed into the x-ray AEC control device by the x-ray system manufacturers, provides a generic relationship to the imaging medium. Medical Physics groups are increasingly aware of the need for greater accuracy in the provision of AEC kVp compensation, as evidenced by recent articles and presentations in the medical physics field (Grieg et al 2005).

A series of standard AEC tests was carried out on several x-ray machines of the same manufacturer at Christchurch Hospital, in order to determine their kVp response characteristic with CR image processing systems.

5.2 AEC optimisation with CR

The wide exposure latitude of a CR imaging system, as described in section 4.7, has created uncertainties in optimising the AEC exposure target level. The requirement is to produce the best possible image quality whilst using the lowest possible dose to the patient (Lu et al 2003). The extreme ends of the CR dose response characteristic should be avoided due to the effects of dose non-uniformity. In this regard CR is similar to a screen-film system. One possible solution may be a setting that exhibits minimal image noise visualisation. This setting is the only verifiable value where the

exposure dose applied will be as low as possible while still providing satisfactory image quality. The Medical Physics Monograph 30 (Goldman and Yester 2004) suggests that the limits and limit parameters applicable to screen-film systems may not be appropriate for CR. It proposes that EI limits could be based on just noticeable differences in noise levels observed in images with low EI values and radiation dose limits for images with high EI values. However this type of assessment is subjective and is therefore inherently less accurate than a quantitative approach and its setting cannot be absolute.

5.2.1 AEC dose set-point with CR

The Medical Physics group at Christchurch Hospital uses the following test procedure to set up or verify the AEC dose set-point. A PEP of 2 × 75 mm thick Perspex (Lucite) slabs is placed on the x-ray table or against the erect Bucky such that it covers all AEC chambers in the Bucky assembly. The x-ray tube is positioned at the specified SID (usually 100 cm) according to the Bucky specifications. Beam energy is set to 81 kVp and the beam collimated to 75 mm beyond all edges of the AEC chambers. The central AEC chamber only is selected to control the exposure. An AEC exposure is performed and the dose recorded using a 15cc ion chamber placed at the centre of the Bucky tray. The measured dose under these test conditions is required to be 4.5 ± 1 μGy (0.5 ± 0.1 mR). The AEC dose control circuit is adjusted by the service engineer to achieve this required dose. A CR cassette exposed under the same conditions should record an exposure index of 1710 ± 100 EI. This AEC setup method and procedure at the hospital has become the protocol by which all AECs are calibrated.

This protocol was derived from a compromise of recommendations between the radiology group, Medical Physics department and the equipment manufacturers. The AEC dose set-point for the Kodak Lanex medium film in use prior to the change to a Kodak CR system technology was not defined by a fixed dose value but by a range of OD. However, analysis of results from local x-ray facilities which have converted from screen–film to CR has shown a dose increase of approximately 50% with CR. Part of the rationale for the increased value of the dose set point for the Kodak CR system derives from the reduced absorption efficiency of the CR system. CR systems are generally considered to have an absorption efficiency of half that for 400 speed radiographic film systems. For this reason, CR is considered equivalent to a 200-speed radiographic film system (Goldman and Yester 2004). The Kodak Lanex medium T-

MAT G RA film used at the hospital, prior to the inception of CR, has an intrinsic speed of between 250 and 300.

5.2.2 Optimisation procedure for AEC with CR

Typically the setting of the AEC kVp compensation to match the response of an image medium is controlled by the algorithm supplied by the equipment manufacturers and installed at the time of commissioning of the x-ray machine. Each x-ray machine of this manufacturer has the same algorithm installed. AECs set up in this way perform satisfactorily but due to variations in x-ray machine performance and perhaps CR PSP manufacturing variations, are not necessarily optimised.

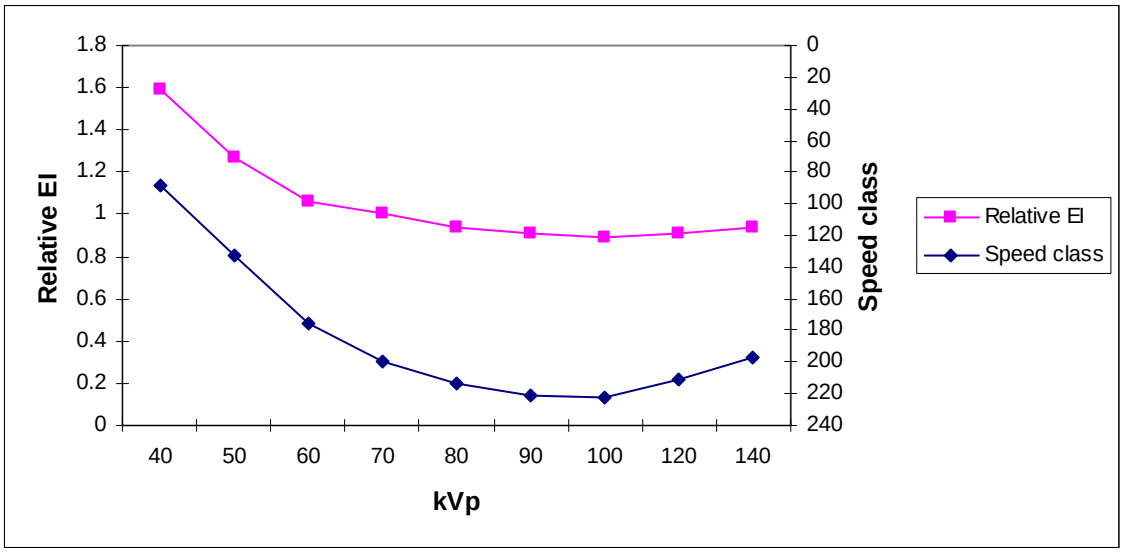

Figure 5.1 Philips AEC kVp compensation

Once the dose set-point at 81 kVp for the AEC has been set up as explained in section 5.2.1, the exposure dose applied for all other kVp settings over the clinical kVp range should be adjusted by the service engineer to provide the same image EI value as obtained at 81 kVp. The engineer adjusts the AEC kVp response according to an adjustable lookup table in the AEC control software. Figure 5.1 shows the AEC control values applied to a Philips x-ray machine in two different ways. The speed class is an index related to the speed of screen - film response. The definition of speed class states that a speed class of 100 is accepted as being represented by an air kerma of 11.1 µGy. Therefore an image plate requiring 2.8 µGy (11.1 µGy / 4) to achieve the standard optical density (OD) = 1 above the base plus fog values has a speed class of 400 (Heggie et al 2001). CR is generally considered to have a speed class of 200 and the response shown in Figure 5.1 can be compared to this value. A higher value for a

speed class implies a reduction in applied dose compared to a lower speed class value. Philips use a reference to speed class values to determine the correct AEC calibration adjustment for the type of x-ray machine used for this thesis. The relative EI is an index based on the relative effect of kVp on the EI values recorded for test images and is dependant on the AEC settings applied for each kVp.

The speed class curve shows data for the existing AEC kVp compensation algorithm. The relative EI curve shows the data for the optimised AEC kVp compensation algorithm. The relative difference between these two curves is a visual indication of the differences in the AEC settings between the two test scenarios. The algorithm data are stored in the AEC software for the Philips x-ray machines and also recorded by the engineer on his laptop computer for each machine. Other types of machines may have different arrangements to store the AEC setup values.

For this thesis a process of trial and error was used to obtain the optimal result for EI consistency. The ideal result is a consistent EI response over the clinical kVp range and, to a first order, a consistent noise response.

5.3 Determination of AEC EI test limits with CR

A testing protocol is required for assessing AEC functionality with any imaging medium. When CR is the imaging system, this protocol should be determined from the unique characteristics of this technology although the protocol for similar existing technologies may provide useful guidelines. An example of such a process is the translation of the exposure parameters accepted for the OD variation limit used with screen-film systems, to CR systems. The radiographic film variation limit is 0.2 OD for AEC exposure reproducibility over the clinical range of kVp and patient thickness. The dose range to achieve a 0.2 OD variation can be derived from test exposures. CR plates can then be exposed to this dose range in order to determine the equivalent EI range. This derived EI range can then be considered as the EI variation limit for AECs used with CR.

This translation process has already been explored and an EI variation of ± 70 index values has been derived for Kodak CR systems (Wilkinson and Heggie 1997). Due to CR's wide exposure range and the complementary effect of digital image enhancement techniques, a wider EI range for AECs using CR imaging could be tolerated. The resulting ± 70 index point variation is less than 2% of the range of possible EI values available in the Kodak system. However increasing this limit would

compromise the purpose of an AEC to minimise dose while maximising the control over image consistency. The derived ± 70 index point limit should therefore be the maximum variation allowed, consistent with the 0.2 OD variation allowed for screen-film systems.

Having gained an understanding of EI limitation for image consistency with CR systems, we should determine if this limit can be reduced further. An optimised kVp compensated AEC should enable a greater consistency of image and EI response. The range of EI values obtained for test images over the kVp range under these conditions should decrease, therefore the theoretical range of the EI limit should be able to be decreased.

5.4 X-ray beam standardisation for test functions

In the past there has been minimal standardisation of beam energy and filtration settings used by medical physics groups around the world to test and evaluate x-ray systems. This is characterised by a variety of test methodologies and exposure levels. A beam energy of 81 kVp is used for the AEC dose set-point and for much of the AEC assessment testing at the Christchurch hospital. This energy has not been set as a standard but is commonly quoted when used for the purpose of AEC testing. I have observed that some medical physics groups use a PEP such as Lucite while others prefer the use of copper or aluminium as the beam-filtering medium for AEC testing. The latter filter types produce minimal scatter and perform well for acquiring measurements to accurately track changes in x-ray or imaging performance over time. However, they do not simulate clinical exposure conditions where scatter is an inherent part of the process. If the purpose of any x-ray testing procedure is to simulate the effects of a patient equivalent x-ray beam spectral distribution then the use of some type of PEP is desirable (Fetterly and Hangiandreou 2000). Perspex was used in the experimental tests performed for this thesis due to its ability to emulate, as far as possible, the effects of clinical x-ray exposures on the performance of an AEC device.

Chapter 6

Developing a test procedure to optimise AEC performance with CR

6.1 Introduction

A range of tests was required to derive the AEC response characteristics of the existing AEC setup for the x-ray machine. The test sequence was then repeated using the same AEC which had been optimised for the kVp response of the image medium. The two sets of response characteristics were analysed and compared to determine the benefits of optimising AEC kVp compensation. The EI was recorded for each test exposure of each AEC scenario. Each test exposure was repeated and the exposure dose at the plane of a CR cassette, located in the Bucky, recorded. All exposures were performed on a single AEC equipped x-ray machine to avoid inconsistencies due to variations in operation and performance of different machines even of the same manufacturer and type.

The test exposures were performed using 18 cm × 24 cm CR cassettes. The cassettes were oriented with their longest axis vertically in the centre of the erect Bucky cassette tray. To maintain consistency in the test procedure and therefore achieve comparable results it was important to adhere to this type of strict procedural regimen. The test exposures were carried out by selecting only the central AEC chamber, both for consistency and for its relevance to the procedure for determining the AEC dose set-point. The middle of the central chamber physically aligns with the centre of the Bucky cassette tray.

6.2 The selection of Ionisation Chamber

The device used to measure dose to the cassette tray must satisfy two requirements. It must be able to be located consistently in the confined space in the centre of the Bucky cassette tray, and it should have some directional selectivity to the x-ray primary beam to minimise its sensitivity to scatter radiation.

There are many types of ion chamber available to the medical physicist, each with its own operating characteristics to match the requirements of the application. Two of these types of ion chamber are available at Christchurch Hospital. The first of these is the Capintec graphite lined, parallel plate and Omni directional cylindrical model

shown in Figure 6.1. It is ideal for Computed Tomography (CT) where the x-ray tube rotates about the patient tunnel or “doughnut”. The design allows for the collection of all x-ray radiation generated in the CT tube’s 360 degree rotation. The chamber’s susceptibility to all scatter cannot be controlled due to its design requirement to collect dose from any direction. It could however be accommodated within the confined space of a Bucky tray for the purpose of the test procedure.

NOTE:
This figure is included on page 59 of the print copy of the thesis held in the University of Adelaide Library.

Figure 6.1 A graphite lined parallel plate pencil chamber (Reproduced courtesy of Radcal Corporation).

The second ion chamber available was the Inovision Model 96035B ‘pancake’ type 15 cc ion chamber. As discussed in section 6.3, this chamber satisfies both requirements.

6.3 Profile of the Inovision ion chamber

The Inovision Model 96035B ion chamber shown in Figure 6.2 has parallel plate (collector and guard) geometry, constructed of air equivalent plastic, vented to the atmosphere. The guard electrode is designed to minimise the effects of scatter. The chamber is designed to measure incident radiation perpendicular to the entrance window. It has a narrow angular dependency such that the value recorded for any radiation within 8º of perpendicular is within 1% of the perpendicular value for the same incident radiation. X-ray photons pass through and are absorbed by the ion chamber materials and the air within the chamber. The main x-ray absorption takes place in the chamber window, collector and walls, because of their higher density compared to air, causing the emission of high-energy electrons. These interactions with the chamber structures produce ionised tracks consisting of lower velocity

electrons and air ions. A positive 300 volt bias potential is applied to the collector which separates the ion and electron clouds and sweeps the electrons out of the air volume and into the electrometer before they recombine again. The guard electrode is also connected to the 300 volt bias potential. The electrons captured by the collector electrode form an electrical charge that is measured by an electrometer. The measured result is displayed, in international units of radiation, on the display panel of the electrometer.

This type of ion chamber, although designed to reduce the effects of scatter radiation on dose measurements, is still affected by it.

Figure 6.2 The Inovision Model 96035B 15cc Ion Chamber (courtesy of fluke biomedical)

The Inovision instrument and ion chamber has an annual calibration check performed by the National Radiation Laboratory (NRL) who issues a calibration certificate with the test results.

6.4 Ion chamber test setup

X-ray scatter from any source and direction causes problems with exposure measurement accuracy and consistency. Scatter that is in the same direction as the

primary beam is called forward scatter. This type of scatter is unavoidably detected by both the imaging medium and measuring ion chamber. However, insofar as it impacts on the imaging medium, it forms part of the dose to the medium and therefore to the measuring instrument.

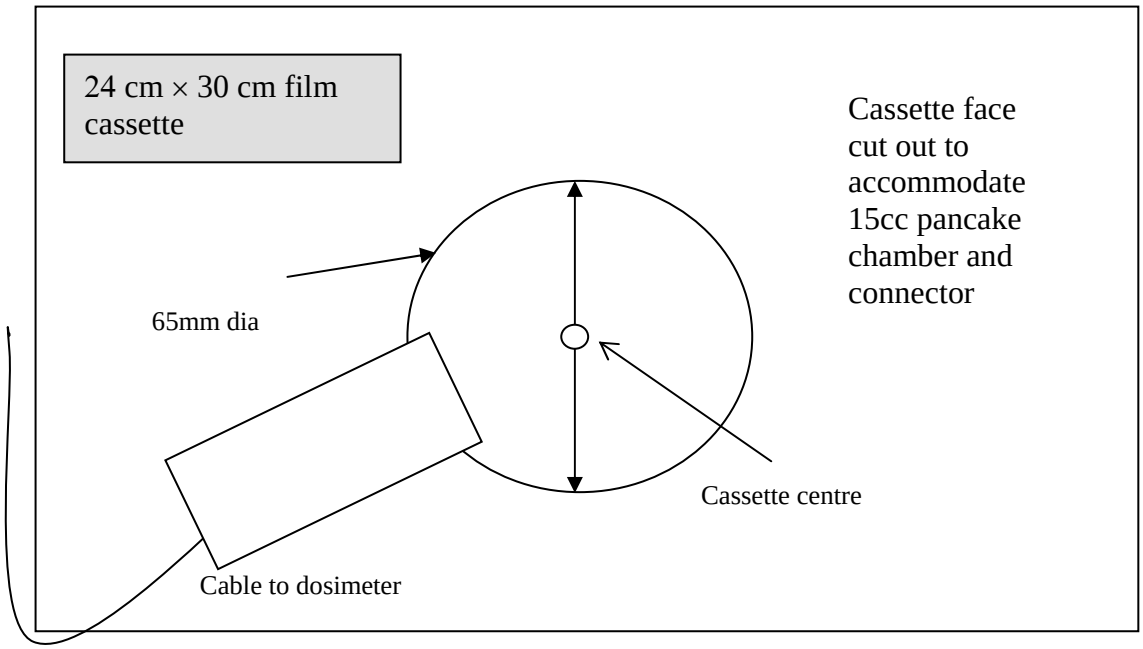

Figure 6.3 Test cassette layout

A test set-up was sought to measure the clinical AEC dose to a CR cassette by locating the measuring ionisation chamber in the same plane as a cassette placed in a Bucky tray. The test setup was required to minimise the effects of backscatter on measurement accuracy. The concept of using a redundant film cassette to accommodate and locate the ion chamber within the Bucky tray was developed by a work colleague Stephen Rofe. He also constructed a prototype, based on the drawing shown in Figure 6.3, using a redundant 24 cm × 30 cm Kodak film cassette which, subsequent to operational tests to prove its effectiveness, was used in the recording of dose measurements for this thesis.

The face of the cassette which faces the x-ray tube was cut out to accommodate the ion chamber and its connector. The active face of the ion chamber is located in the geometric centre of the cassette and lies flush with its surface. The cassette's internal structures including screens were removed from the test cassette. The 2 mm aluminium rear panel was also cut out to the shape of the ion chamber to enable the

placement of various materials in order to test their effectiveness in reducing backscatter as described in section 6.4.1.

6.4.1 Minimising back scatter in the test setup

Scatter radiation results from interactions of the primary x-ray beam with objects in its path and depends on the energy spectrum of the primary beam. Energy is transferred by these interactions so that the scattered radiation has less energy than the primary beam photons. An illustration of the x-ray spectral response curve for Tungsten, the most common x-ray target material, is given in Figure 6.4 for a set accelerating voltage of 100 kVp.

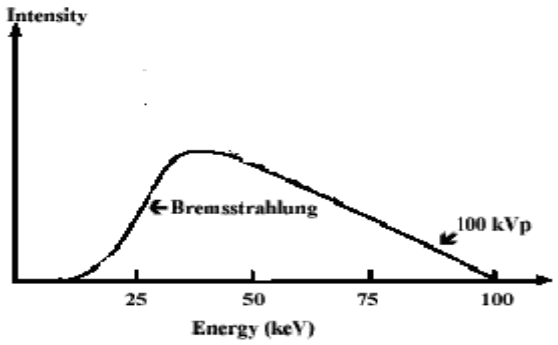

Figure 6.4 X-ray spectrum for tungsten target

The energy spectrum for this target material has a keV range of approximately 12 keV – 100 keV. For clarity the characteristic radiation peaks of the tungsten spectrum have been removed. Depending on the interactions of the primary beam photons with objects in their path, the x-ray scatter produced may have energies anywhere below the maximum energy. By definition the scatter energies cannot reach the maximum energy of 100 keV.

A significant part of the scatter incident on any dose measuring instrument is called backscatter. This backscatter is generated from x-ray photon interactions with materials located behind the ion chamber. Backscatter can be generated in all directions. Since there is no grid to minimise the effects of backscatter to the image medium, it is detrimental to image quality.

In order to minimise the backscatter component of the dose to the ion chamber, it was essential to determine the most effective backscatter attenuator to mount on the rear of the test cassette containing the ion chamber. A series of tests was carried out using a

fixed exposure to determine this factor. The attenuating medium was attached over the rear of the cassette, completely covering the rear of the ion chamber. For consistency the test exposures were carried out with the same exposure parameters used for setting up the dose set-point for the AEC given in section 5.4, namely a beam energy of 81 kVp, an SID of 1000 mm and a 150 mm Perspex PEP phantom. The central AEC chamber only was selected on the x-ray machine's operator panel.

Since the dose reading includes incident radiation and backscatter radiation, the attenuating material which results in the lowest recorded dose reading has the best backscatter reduction characteristic.

Cassette backing material	**Material Thickness (mm)**	**Measured dose (µGy) (Average of three readings)**
Aluminium (Al)	1	5.2 ± 0.1 µGy
Aluminium (Al)	2	5.2 ± 0.1 µGy
Copper (Cu)	1	5.7 ± 0.1 µGy
Copper (Cu)	2	5.7 ± 0.1 µGy
Lead (Pb)	1	5.5 ± 0.1 µGy
Lead (Pb)	2	5.4 ± 0.1 µGy
None		5.7 ± 0.1 µGy
Chamber positioned in Bucky without test cassette or backing		5.7 ± 0.1 µGy

Table 6.1 The effectiveness of various attenuators to reduce the backscatter incident to an ion chamber placed within a Bucky cassette tray.

Table 6.1 shows the recorded dose results for exposures to the chamber with various metal attenuators placed behind the ion chamber for backscatter reduction. The most effective attenuator for backscatter under the test setup condition described was 1 mm or 2 mm aluminium. The dose measured using this backscatter control medium was 5.2 ± 0.1 µGy. The value derived corresponds to the measured value of the AEC dose set-point and is within the dose set-point limit of 4.5 ± 1 µGy.

Kodak uses 2 mm aluminium as the support medium for the PSP and to minimise the effects of backscatter to PSP material. Within experimental error the difference between the use of 1 mm aluminium and 2 mm aluminium for backscatter reduction was insignificant. Since Kodak uses 2 mm aluminium for its CR cassettes, this option was also chosen for the experimental test procedures for this work, both for its proven reduction of backscatter and for its similarity to the physical design of Kodak CR cassettes.

6.5 X-ray Bucky arrangement in test set-up

Figure 6.5 is a photograph of a typical Bucky assembly as used in the experimental work. The anti scatter grid is located on the fixed part of the Bucky, shown on the left of the photograph, just behind the front cover showing the layout of the AEC chambers. The AEC chambers are also located on the fixed part of the Bucky and are positioned just behind the anti-scatter grid. The film or CR cassette is clamped onto the cassette tray shown on the right side of this photograph. The tray is slid into the fixed Bucky assembly. This locates the CR cassette behind the AEC chambers and anti scatter grid.

Figure 6.5 Bucky cassette tray

6.5.1 The anti-scatter grid

The antiscatter grid is a very effective device for the reduction of scattered radiation incident on the front of the CR IP. The grid is constructed as a flat plate composed of a series of uniform lead strips interposed with some material transparent to x-rays. The grid is specified by several factors that relate to the height of the lead strips, the distance between them and the number of strips per centimetre. The lead strips are

oriented along the direction of the x-rays emitted from the x-ray tube and designed to be focussed at a fixed SID.

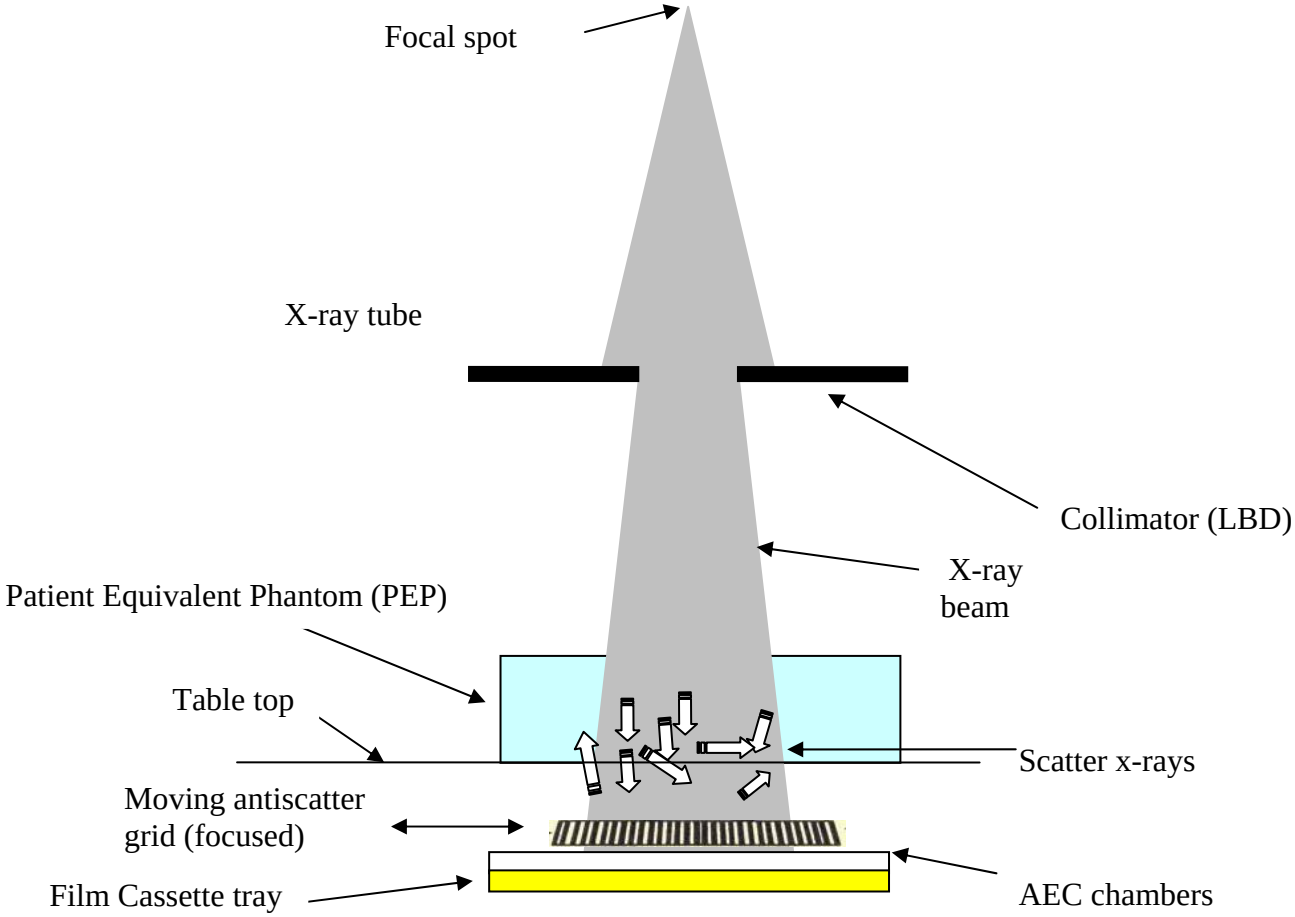

Figure 6.6 Potter Bucky / moving grid Bucky

Figure 6.6 is a diagram of a Potter moving grid Bucky. It was developed in 1920 by Hollis Potter and uses the principle of reciprocating (back and forth) grid motion not only to reduce the effects of x-ray scatter but also to reduce the visibility of the grid lines on an image. Moving grids remove scattered radiation very effectively while blurring out the image of the grid lines themselves. However, they introduce several disadvantages: they are more costly, subject to greater failure incidence due to their mechanical construction and degrade image density. The latter problem requires that the patient dose be increased to maintain image density and quality.

Essentially, only those x-ray photons emitted from the x-ray tube or exiting a patient in the same focus direction as the grid structure lines are able to pass through the grid and contribute to the formation of an x-ray image. This places a high degree of importance on setting the SID correctly, to match the grids focus distance, to avoid grid cut-off effects. Any scattered radiation that may otherwise have contributed to

image noise is absorbed in the lead strips of the grid and does not contribute to the formation of the x-ray image. Prior to the development of the moving grid, the benefits of the stationary version were well appreciated even though the grid lines themselves may have been visible in the resulting images.

6.6 The test procedure and measurement accuracy

For the functional AEC tests, the AEC dose response was measured and the exposure index recorded for all test exposures, using the AEC test set-up explained in section 5.2.1. The tests were carried out over the clinical range of x-ray spectra 60 kVp to 125 kVp and PEP thicknesses of 75 mm, 150 mm, 225 mm and 300 mm Perspex, using an SID of 140 cm for the erect Bucky which corresponds to the Bucky grid specifications. The PEPs were placed directly in front of the Bucky, covering all three AEC chambers. The x-ray beam was collimated to form a 300 mm × 300 mm radiation field size at the Bucky.

For consistency, a single x-ray machine was used in the collection of all data for these tests. The x-ray machine was a standard Philips Optimus 50 equipped with a table Bucky and an erect Bucky, both of which incorporate a typical moving grid mechanism. All AEC doses were measured at the plane of a CR cassette, when placed in the Bucky tray, using the test cassette described in section 6.4, with 2 mm Aluminium in place as the cassette anti back-scatter material. A single Kodak CR 900 reader was used to process the test images. The EI of the homogenous images were recorded from the ROP after each exposure.

The Inovision dosemeter accuracy has been certified by NRL as – 1 ± 0.1% at 60 kVp, + 1 ± 0.1% at 80 kVp and + 3 ± 0.1% at 100 kVp. A series of 20 exposures using the same test parameters was carried out to determine the reproducibility of the x-ray machine. The measured dose values were calculated to have a maximum deviation of ± 2.5% from the average. All EI values were calculated as having a maximum deviation from the average value of less than 1%. These measurement uncertainties are much smaller than the variations observed between mean values for the different test settings.

6.7 Summary

Tests were conducted on a single Philips Optimus x-ray machine equipped with AEC. The service engineer was requested to provide a switchable option which enabled the

AEC to perform using the generic algorithm or using the experimentally derived algorithm which optimally matches the kVp response of the CR imaging medium. This switching option was set according to which operating mode was required. Chapter 7 provides the results of tests conducted using each of these scenarios.

The initial series of tests were performed with the generic AEC kVp compensation set on the x-ray machine. They were then repeated with the x-ray machine set for optimal AEC compensation designed to match the kVp response characteristics of the Kodak CR imaging medium as described in section 5.2.2. All tests where recording of image data was required used an image processing delay of 60 ± 10s between exposure to x-rays and the placement of the CR cassette into the CR processor.

Chapter 7

Test results: the rationale for an optimised AEC

7.1 Introduction

The original idea that began this work was an investigation into the transferability of current protocols for AEC functionality testing with screen- film imaging systems, to CR imaging systems. This concept has evolved to become an investigation into the optimisation of AEC control to ensure the highest level of image consistency over the clinical kVp range. In order to perform this investigation an experimental procedure was developed which provided a repeatable test setup to record the results for both the current AEC control algorithm and for an optimised AEC. This chapter is the culmination of this development, providing the experimental results with discussions pertaining to the benefits of optimised AEC control.

7.2 Specific test considerations

A result for the largest PEP of 300 mm Perspex at 60 kVp is missing from all the test results. In practice an x-ray machine set to AEC under these conditions would not be able to achieve the required dose to the AEC detectors before the maximum allowable time had expired or the maximum mAs reached. The maximum allowed AEC exposure time is 6 s and / or 600 mAs. These AEC exposure limits are imposed by international standards as a safeguard to protect patients from overexposure should the machine timer fail to terminate an exposure normally. Additionally this low kVp exposure is considered non-clinical since it simulates a low energy exposure to a large patient. A 60 kVp exposure provides insufficient energy to penetrate such a large mass and produce an image with good contrast.

The error bars shown on the following test results for dose measurements relate to the dosemeter accuracy stated in section 6.6 from a report by NRL. The image EI accuracy is derived from the results from experimentation with image processing times given in section 4.12.

7.3 Test results for an AEC with generic kVp compensation applied for CR

The histograms of Figure 7.1 and Figure 7.2 are the results of tests conducted on the x-ray machine with the AEC set to generic kVp compensation. They show the dose profile and corresponding IP exposure index (EI) response, respectively, over the clinical kVp range 60 kVp to 125 kVp and PEP thicknesses of 75 mm to 300 mm Perspex simulating exposures over the normal range of patient sizes.

The AEC dose response shown in Figure 7.1 exhibits a dose average of 0.65 mR with a maximum variation from this average of 0.17 mR representing 26% dose variability.

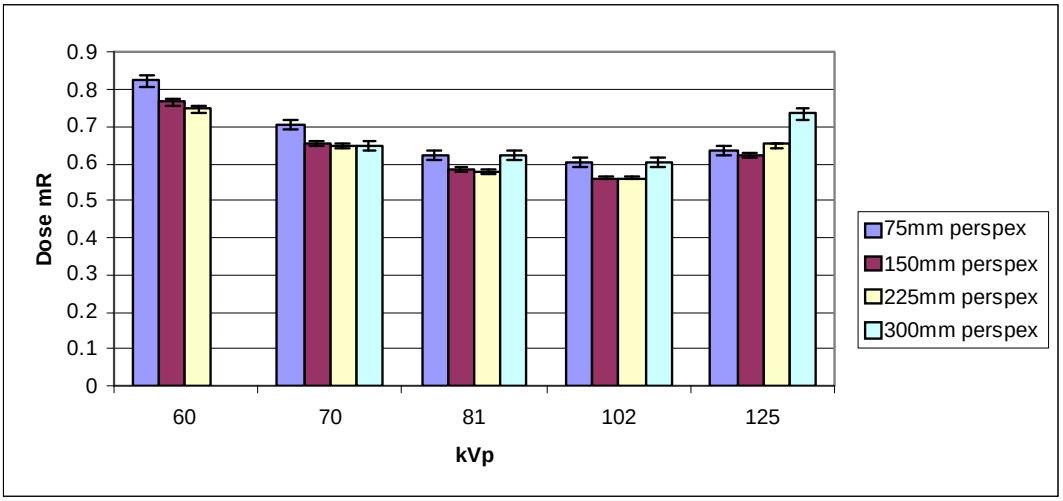

Figure 7.1 Generic AEC response to kVp and PEP: Dose response

The EI response to changes in kVp and PEP thickness plotted in Figure 7.2 shows a similar response pattern. Scatter in the absorber material is perhaps the most important factor which influences the EI pattern deviations from the dose pattern. As the exposure kVp increases, the scatter in any absorber material in its path increases. The dose to the IP decreases and the AEC prolongs the exposure to maintain the dose to its sensors. This results in a higher dose being recorded by the measuring dose chamber which is placed in the same relative position as the AEC's centre chamber. The IP is itself a dosemeter but its response is kVp dependant and the reported EI value is the average pixel value over the entire IP. The overall effect is a reduction in the reported EI values for increasing kVp and for the scattering effects due to increasing absorber thickness.

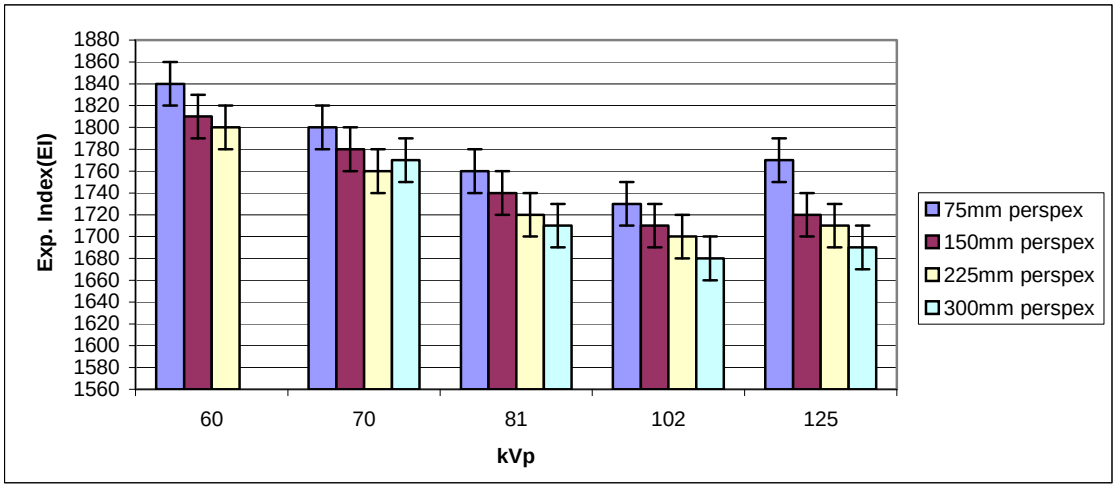

Figure 7.2 Generic AEC response to kVp and PEP variability: EI response

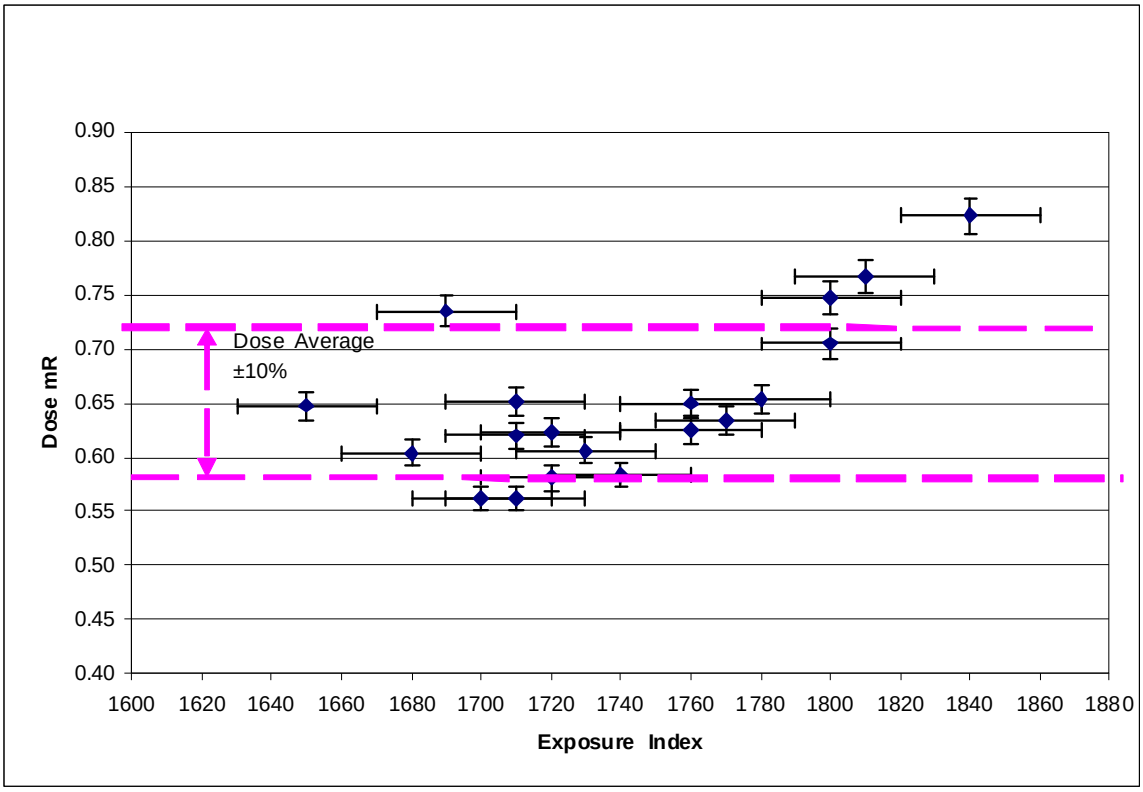

Figure 7.3 Generic AEC response to kVp and PEP: Dose and EI distribution

The average EI value was 1740 with a maximum EI variation from this average of 100 index points. This variation exceeds the theoretical ± 70 EI limit, as described in section 5.3, of a consistent response to changes in PEP thickness over the clinical kVp range. While these results for this thesis were obtained from a single x-ray machine they are typical of several AEC equipped x-ray machines at the hospital. They

represent the status of the generic AEC kVp compensation response before the experimental kVp compensation was installed.

The graph in Figure 7.3 shows the dose and EI distribution of the data from Figure 7.1 and Figure 7.2. It illustrates that the generic AEC kVp compensation algorithm produces a dose and EI profile which is inconsistent over the clinical kVp range. A 10% dose limit (shown by the dashed magenta lines) placed about the average dose value of all the measurements highlights the fact that several measurements fall outside this range depending on error values. The EI range over these measurements was 190 index points with an average EI of 1740 resulting in a range of 1740 ± 95 EI. Some values lie outside the theoretical limit of ± 70 EI referred to in section 5.3, even allowing for the error values. The relationship highlighted by this set of results will be used later to compare with the relationship produced when the AEC has been optimised to match the CR response to kVp.

7.4 Test results for an AEC with optimised kVp compensation applied for a CR imaging system

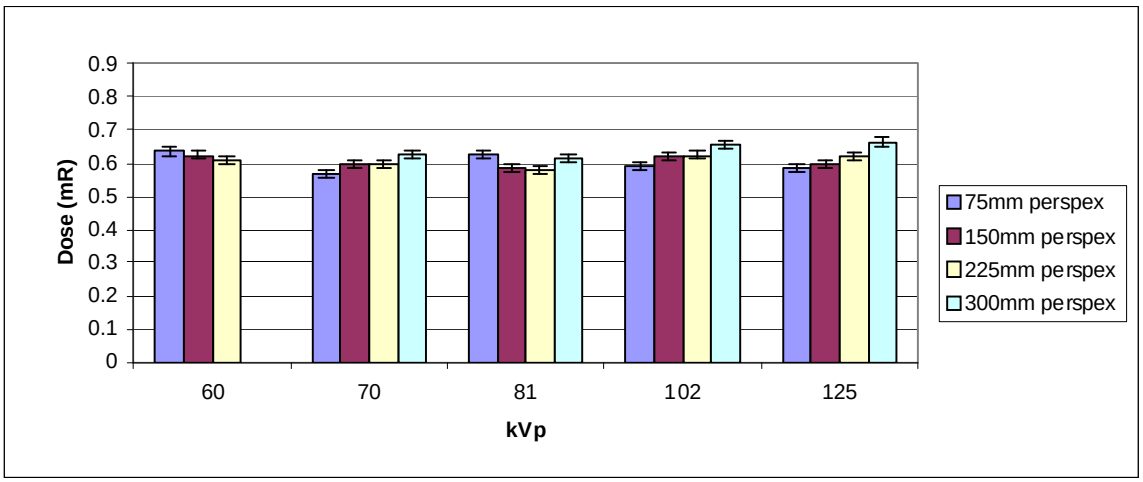

Figure 7.4 AEC optimally kVp compensated: Dose response

The histograms shown in Figure 7.4 and Figure 7.5 are the results of a repeat of the tests conducted to derive the results for the histograms in Figure 7.1 and Figure 7.2 but with optimised kVp compensation applied to the AEC. This is the process by which an AEC is adjusted to optimally match the kVp response of the imaging medium as described in section 5.2.2.

The dose average for the results shown in Figure 7.4 is 0.612 mR with a maximum dose variation from this average of 0.051 mR representing 8.3% variability. The EI response to changes in kVp and PEP shown in Figure 7.5 has an average EI of 1715 with a maximum variation from this of 35 index points.

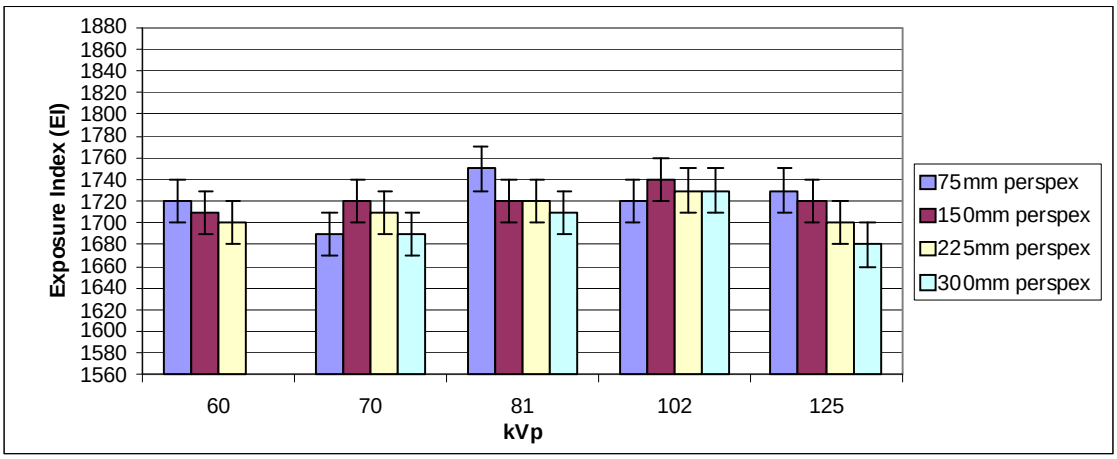

Figure 7.5 AEC optimally kVp compensated: EI response

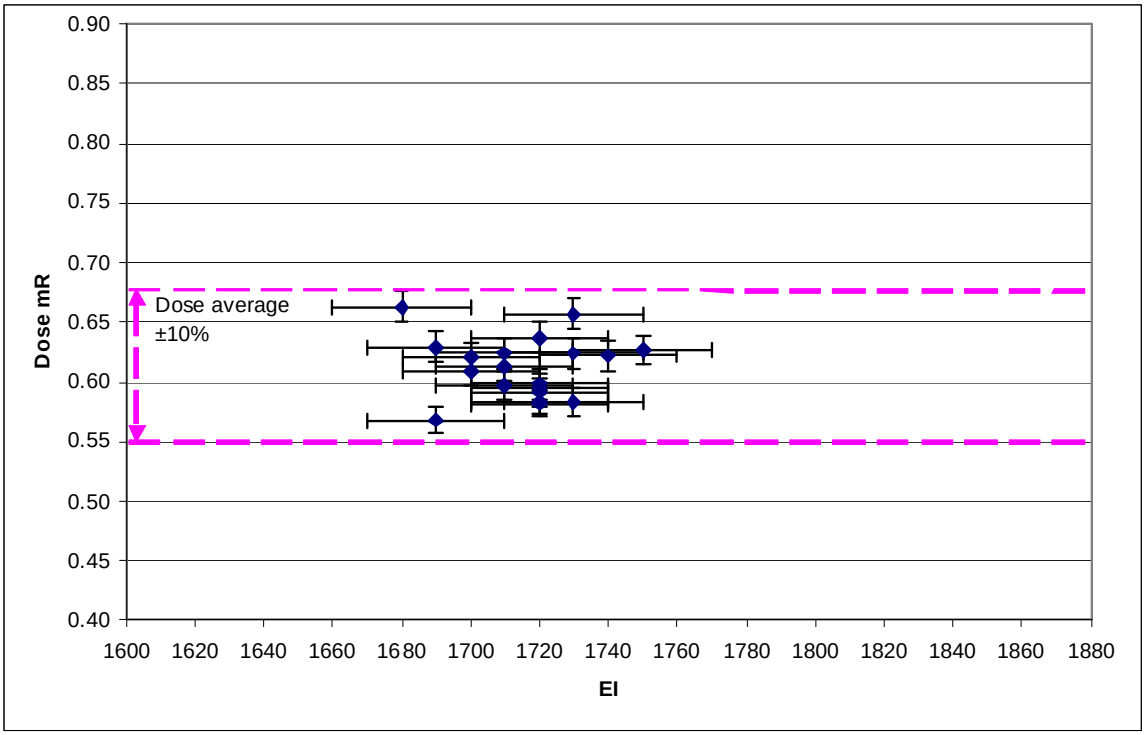

Figure 7.6 AEC optimally kVp compensated: Dose and EI Distribution

The graph of Figure 7.6 shows the dose and EI distribution of the data from Figure 7.4 and Figure 7.5. It illustrates that the AEC, optimised to match the kVp response of the image medium, produces a dose and EI profile that approaches the ideal situation of a

constant dose and EI over the clinical kVp and PEP thickness range. There are many exposures around the ideal 1710-1720 EI range. Taking into account the error, most measurements fall within a 10% dose range about the average dose of 0.612 mR shown on Figure 7.5 by dashed magenta lines. The EI range, over all these measurements, was 70 index points with an average EI of 1715 corresponding to a variation of 1715 ± 35 EI.

7.5 Evaluation of Dose and EI responses

The results from section 7.4 show that optimal adjustment of the AEC system to match the characteristics of a Kodak CR imaging system improves the consistency of the EI and dose responses. The generic algorithms for CR as currently applied to the AEC systems do not provide the optimum results that are attainable using the protocol proposed in this thesis. The experimental results from optimising AEC kVp compensation have shown a dose variation, over the test kVp range, of less than ± 10% of the value at the AEC calibration dose-point set at 81 kVp. In achieving this result the range of image EI values over all exposures was constrained to within ± 35 EI values. This is much better than the current EI tolerance limit of ± 100 EI for AECs using the generic algorithms. The attainable range of EI is also half the range of ± 70 EI values calculated from the dose variations for the screen-film imaging medium OD limit of ± 20% OD, as described in Section 5.3.

An optimised AEC is capable of producing a measured dose to an image plate variance of less than 10%. The measurement of this dose variance is therefore a measure of the accuracy of the AEC optimisation process. Therefore the measurement of AEC dose to the image plate should be able to perform as a tool to determine the performance of an AEC.

Chapter 8

Image Quality comparison of AEC setups

8.1 Image Quality testing

Having established that better optimisation of AEC functionality with a CR imaging medium can be achieved by applying appropriate AEC kVp compensation, it is necessary to determine the effect of this compensation on the system image quality. In any radiographic imaging system, image quality can be determined by assessing contrast detail and spatial resolution performance. These in turn are dependent on:

- Image contrast of the system
- Unsharpness which is determined from the spatial resolution limit measurement
- System noise
- Quality

8.2 Contrast-detail test

The Leeds TO. 20 contrast-detail test object is commonly used by Medical Physicists for the task of determining system contrast response. To quote a passage from Workman and Cowan (1993) “The use of contrast-detail test objects has become a widespread practical approach to assessing the image quality of radiographic systems.” The Leeds TO. 20 test object is a circular plastic construction, 250 mm in diameter and 9 mm thick, with embedded metallic details with a range of diameters and x-ray contrasts. A representative image of the test object layout is shown in Figure 8.1. There are 144 details in all, comprising twelve sizes of detail ranging from 0.25 mm to 11.1 mm in diameter, each size detail being present in twelve different x-ray contrasts. The details have been designed to operate at an x-ray beam energy of 75 kVp with additional filtration in the beam of 1.5 mm copper (Cowan et al 1992). When the test object is imaged under these conditions it provides a universal standard for contrast detail testing.

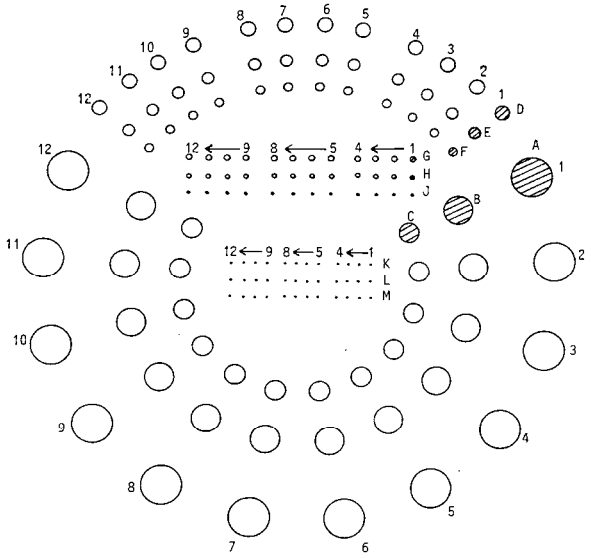

Figure 8.1 Leeds TO. 20 contrast-detail test object radiographic layout

8.2.1 Contrast-detail test description

The contrast-detail test was conducted by exposing a Leeds TO. 20 to x-rays over the clinical kVp range 60 kVp-125 kVp. The test object was placed on the front of the erect Bucky at an SID of 1400 mm from the x-ray focus. Filtration of 1.5 mm copper was added at the x-ray tube to provide the beam energy spectrum specified by the manufacturers of the Leeds contrast-detail test object. The x-ray beam was collimated to cover the entire AEC field. For consistency a single CR cassette was used for all tests and placed in the cassette tray of the Bucky. The resulting images were sent to PACS. To review these images for analysis they were retrieved from PACS to a calibrated computer workstation using the imaging software program called 'E-Film'. Images were viewed under dimmed lighting conditions and windowed and levelled, as explained below, to obtain the best visualisation of the details in the TO. 20 image. The total number of details observed in the image was recorded for each kVp setting for both the generic AEC kVp compensation and the optimally kVp compensated AEC scenarios.

Window and level adjustments for image viewing

Computer based software allows digitised images to be manipulated to enhance image visualisation. The radiographic images from a Kodak CR system are formed using a 2^{12} bit digitisation process, as explained in section 4.8, which provides 4096 individual

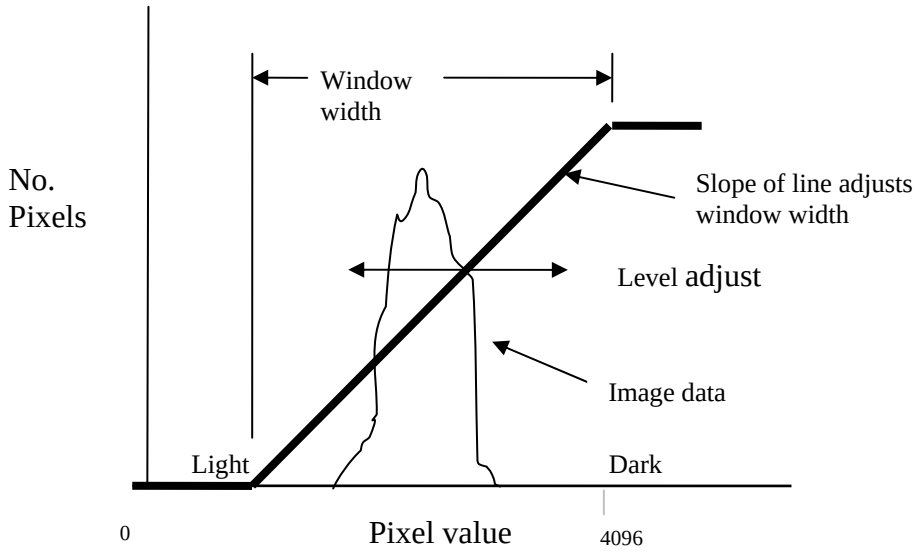

Figure 8.2 The Kodak image histogram

contrast values. Each image pixel will have a contrast value attributed to it once it has been scanned by the CR laser. Figure 8.2 shows the layout of the Kodak histogram. The Kodak image display software package incorporates a histogram which shows the pixel value on the 0- 4096 scale on the horizontal axis and the number of pixels on the vertical scale. The process of applying the full 0- 4096 pixel range to different parts of the available image data is called windowing and levelling. The dark diagonal line in Figure 8.2 covers the range of pixel values available. When the slope of the black line is increased the image component window is decreased such that less of the total image is included in the pixel range. This expands and amplifies small changes in pixel values of the selected image pixel range which has the effect of increasing the image detail visibility. If the thick black line is moved to the left, without changing its slope, the image window remains the same but the image content containing the lower value pixels are highlighted. In this circumstance this means toward the lighter components of the image content. The converse occurs when the line is shifted to the right where the larger pixel values or darker components of the image are highlighted.

8.2.2 Contrast-detail test results

Typically, approximately 60% of the test objects on the test images are observed under normal testing conditions. This level of object visibility provides for sufficient scope to detect changes over time or between different set-ups.

As x-ray energy increases, the probability of photoelectric reactions decrease. Because the photoelectric effect is proportional to the cube of the atomic number (Z) of the

absorber material, this effect serves to amplify the contrast difference between different materials. Compton reactions are dependant on the electron density in a material which is generally constant for the materials which make up the test phantom. On the other hand since the probability of Compton reactions increases with increasing x-ray energy the ratio of Compton to photoelectric events increases with increasing energy, so the range of contrast is reduced. The relative effects of increased scatter at higher kVp also contribute to decreased object contrast. As shown in Figure 8.3 the number of objects visible in the Leeds TO. 20 phantom images decreases as the kVp increases.

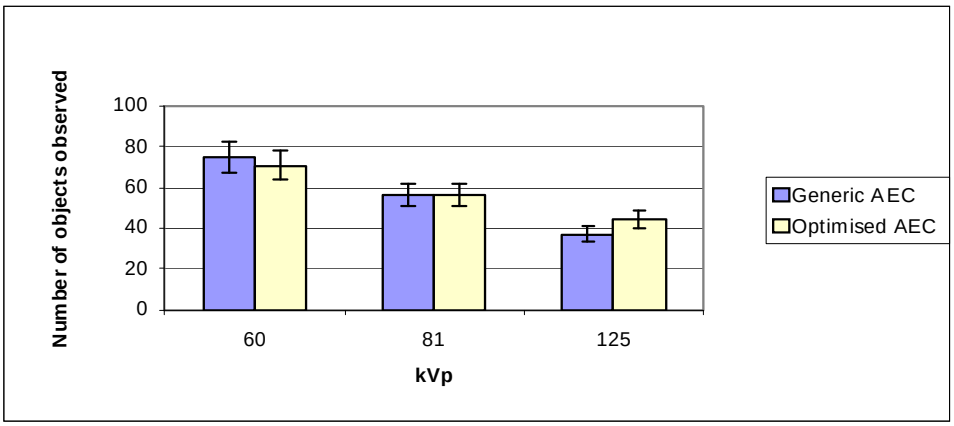

Figure 8.3 Contrast detail comparison between the two AEC compensation scenarios

The variability of the observers' subjective assessment is indicated by the error bars. The reasons for this variability even for a single observer can be understood if slight changes to window and level adjustments are considered in conjunction with the decision process for the observation of each detail object between observations. The differences between the results for each AEC scenario at each kVp setting are not statistically significant.

8.3 The spatial resolution limit test

The spatial resolution limit of an imaging system is defined as the highest spatial frequency of a sinusoidal test pattern that can be visualised. The test pattern phantom is made up of sets of black and white contrast units known as line pairs. The Nuclear Associates spatial frequency test phantom used for this test is shown in Figure 8.4. The spatial frequencies of the bar patterns range from 1 to 4.86 line pairs per mm.

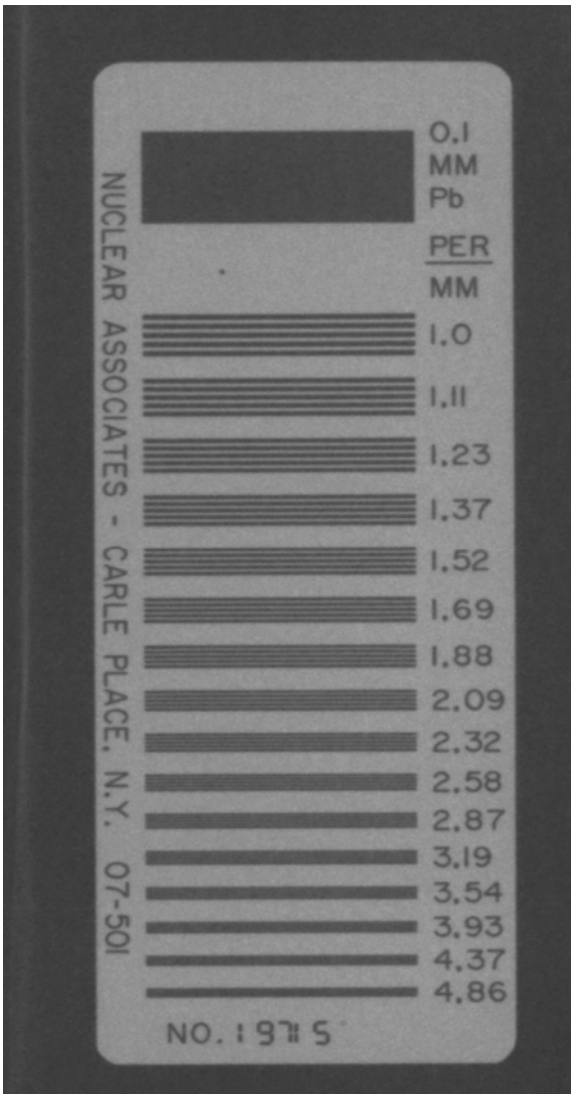

Figure 8.4 X-ray image of the Nuclear Associates spatial frequency test phantom

The accurate representation in digital form of an analogue signal such as the sinusoidal spatial frequencies of the test phantom is based on the Nyquist frequency. The Nyquist frequency is explained in the Nyquist 'Sampling Theorem' (Nyquist 1928). According to the Nyquist sampling theorem, an analogue signal must be sampled at twice the frequency of its highest-frequency component in the signal to be converted into an adequate representation of the signal in digital form. Thus, the "Nyquist frequency" is the highest frequency that can be accurately sampled. It is one-half of the sampling frequency. If sampling of an analogue signal is carried out according to the Nyquist theorem then the reconstruction of the digital signal can restore the analogue signal without error.

Kodak sets its limits for the visualisation of line pair patterns at 90% of the Nyquist frequency as shown in Table 8.1 for each available screen size at a beam energy setting of 75 kVp. This allows a margin from the theoretical maximum resolution given by the Nyquist theorem.

Screen size (cm)	PSP Digital Matrix	Pixel size (mm)	Line pair visualisation, 90% Nyquist frequency
18 × 24	1792 × 2392	0.097	4.6 lp/mm
24 × 30	2048 × 2500	0.115	3.9 lp/mm
35 × 43	2048 × 2500	0.168	2.7 lp/mm

Table 8.1 Kodak CR specifications and spatial resolution limits at 75 kVp

The physical dimensions of a Kodak CR IP are related to its pixel size which is a determinant of its spatial resolution characteristic. At Christchurch Hospital three cassette (IP) sizes are in use. Their dimensions are 35 cm × 43 cm, 24 cm × 30 cm and 18 cm × 24 cm and have pixel sizes as displayed in Table 8.1. These exhibit line pair resolution limits based on 90% of the Nyquist limit ranging from 2.7 lp / mm for the largest pixel size to 4.6 lp / mm for the smallest pixel size.

The spatial resolution of any CR system also depends on such factors as the dimensions of the scanning laser spot and the amount of light scattering within the phosphor. The latter effect depends on the phosphor composition and its thickness. The spatial resolution assessment uses comparative pattern visualisation from test images to determine differences in spatial resolution between AECs with generic AEC kVp compensation and AECs which have been optimally kVp compensated for a CR imaging medium.

8.3.1 Spatial resolution limit test description

The test to determine the limiting resolution of the Kodak CR system used a similar set-up to that used for the contrast detail test. It differed only by the use of 0.5 mm copper + 1 mm aluminium as the beam quality filter placed at the x-ray tube. This filter is used as a beam quality standard by Kodak for some of its test specifications. It is used here not only as a test standard but also to give reasonable image resolution for the higher kVp used in the test procedure. Typically a spatial resolution test is conducted using a single low energy beam of approximately 60 kVp with no filtering.

A single 24 cm × 30 cm CR cassette was used for all tests to maintain result consistency. This was placed in the central position in the x-ray Bucky cassette tray, with the same orientation for each exposure. The line pair test phantom was placed on the front of the erect Bucky over the central AEC field area and oriented so that the length of the phantom lay perpendicular to the long side of the cassette. In this orientation, the phantom lies perpendicular to the laser scan direction for the cassette type used. The CR reader scan directions for this cassette type are illustrated in Figure 8.5. The raster scan lines in this image are slightly skewed, relative to the IP edge in the fast or laser scan direction. This is because the plate undergoes simultaneous laser beam scanning and linear plate translation (AAPM TG 10 2002).

Figure 8.5 CR IP laser scan and plate movement orientations and typical resolutions (courtesy of J.Anthony Seibert, PhD 2003)

8.3.2 The spatial resolution limit test result

The averaged results of three exposures at each kVp setting under each AEC test condition are compared in Figure 8.6. The error bars are based on the subjective observation result obtained ± 1 line pair block of the Nuclear Associates line pair phantom. The variation observed between the three successive readings at each kVp setting was always no more than ± 1 line pair block. The effect of slight variations in each successive radiation exposure on the observed result is insignificant compared to the effect of subjectively derived image assessment.

This implies an error variation of approximately ± 0.4 lp/mm about the observed line pair limit. This error variation is due to the observer' window and level settings between successive readings and the decision process for line pair visualisation.

The subjective response of the observer is influenced by the ambient light in the image viewing area and the distance of the observer from the image surface.

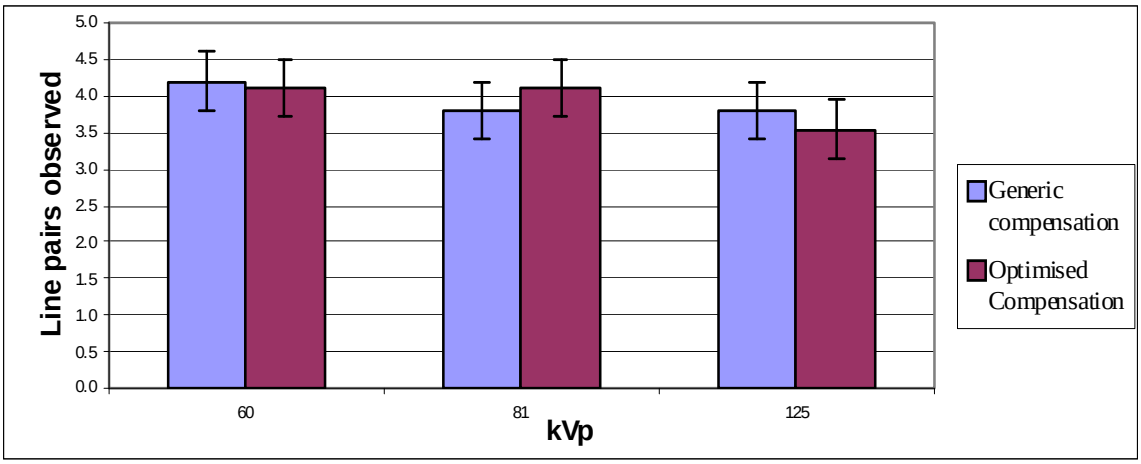

Figure 8.6 The spatial resolution (line pairs) test result

The standard rules given by Kodak apply to the decision making process such that a line pair is considered visible if any parts of the lines are visible throughout their length. There is no statistically significant difference in the spatial resolution obtained with the two AEC compensation scenarios; the maximum variation of 0.3 lp / mm is smaller than the experimental error.

8.4 A comparison of image noise between AECs with generic kVp compensation and AECs with optimised kVp compensation

The SNR characteristic of an image described in section 4.10 has a significant effect on image quality and the visibility of image objects. An optimum image is achieved when the desired signal or image information is maximised while noise sources are minimised. The image produced under these conditions is said to have a high SNR.

A comparison of the relative SNR for the two AEC test scenarios was made using the standard test exposure parameters presented in section 6.6 to obtain a series of exposures. For consistency, a single 35 cm × 43 cm CR cassette was used throughout

this test procedure. For each AEC test scenario, the flat field test images were saved to PACS and reviewed using ‘e-film’ on a PACS workstation. No post processing of the processed images was enabled.

The homogenous images produced were analysed by sampling five regions of interest (ROI) of equal size and recording the pixel standard deviation (PSD) for each area. The PSD is a function provided by the image analysis software and gives the variation in pixel homogeneity due to noise factors within each sample area. The ROIs were taken from each corner and the centre of these images. The PSD provides a measure of image noise within each ROI such that a low PSD value indicates that pixel values are uniform and noise is minimal. A high PSD value indicates that the variation between pixel values in an area is large and that image noise is more significant.

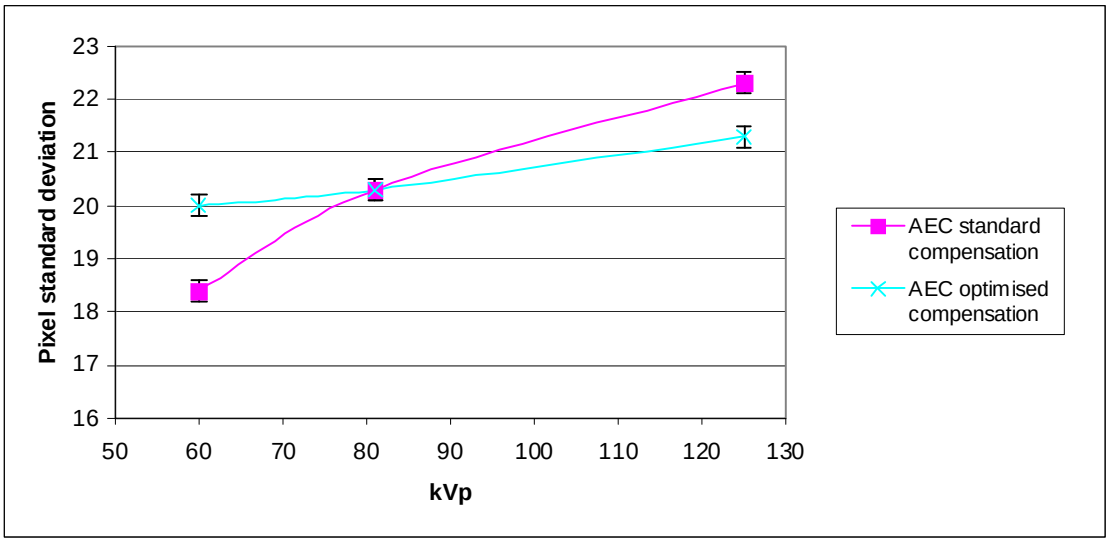

Figure 8.7 Image noise comparison: Generic AEC kVp compensation / AEC with optimised kVp compensation

The average PSD of all five regions of the test images was calculated to provide the data for the image noise results shown in Figure 8.7. The error bars shown on this graph are given to indicate the range of values covered by the measurements at each of the five sampled regions. Although quantum mottle effects increase with increasing kVp, the effects of increased scatter components at higher energies is greater. The combined effect causes an increase in PSD which is evident in the results for both scenarios. The optimised kVp compensated AEC shows a more consistent noise response which is directly attributable to the greater consistency of the optimised AEC dose profile.

The results obtained follow a proposal by Christodoulou et al (2000) that an AEC system is correctly set up when it produces a consistent PSD on homogenous images over the clinical kVp range. The results of optimally setting AEC kVp response for an image medium are consistent with Christodoulou's proposal. Other similar experimental work by Mazzocchi et al (2006) explains a simple AEC calibration procedure for CR systems that functions by correlating the digital signal exposure index with the SNR. The original purpose of AEC was to provide image consistency over a wide range of exposure conditions. EI consistency is a measure of image consistency over the clinical kVp range and is interrelated to improvements to image noise consistency.

8.5 Image quality assessment

The AEC compensation optimisation procedure has not produced significant changes to contrast detail and spatial resolution object visualisation. The comparative SNR test result based on average pixel value variations within selected image areas shows a quantitative improvement to image consistency with an optimised AEC. However its qualitative effect on image quality has been shown to be insignificant.

8.5.1 Clinical confirmation of image quality

From a clinical perspective, the results from the image quality tests indicate that the transition to a compensated AEC protocol would have negligible impact on image performance. Therefore a transition to an optimally kVp compensated AEC can be considered clinically transparent. No change to the current clinical processes or practices should be required to accommodate the results of the proposed new AEC test protocol.

To assure some confidence in this statement, a limited clinical image assessment was carried out. Its purpose was to ascertain if a clinician could discern any significant changes between images produced from an AEC using generic kVp compensation and those performed using an AEC which has been optimally compensated for the kVp response of the imaging medium. A blind study of several randomly selected chest images produced from both AEC test scenarios was presented to a radiologist for assessment. All images were reported as being radiologically similar and acceptable as diagnostic in both image quality and the level of noise present. This result is an indication that any differences between similar images produced under either AEC

compensation scenario have no clinical implications when applied to a Kodak CR system.

Chapter 9

A protocol to test AEC functionality by the measurement of dose alone

9.1 The advantages of AEC optimisation

The AEC optimisation process described in section 6.6 and the experimental results obtained from following this process presented in chapter 7 validate a simplified AEC functionality test procedure using the measurement of dose alone to an image plate. The results from section 7.3 show that the dose profile of an optimised AEC can be constrained within close limits over the clinical kVp range whilst achieving consistent EI results. Image quality from a clinical perspective has been shown to be diagnostically acceptable under these conditions.

Due to the increased consistency of measured dose to a CR image plate as a result of AEC optimisation, the measurement of x-ray dose to an image plate is able to function as a quantitative assessment of AEC performance. An AEC assessed using this method does not change the individual test parameters required to assess overall AEC functionality. It does however change the data acquisition and display function of these test parameters. The data acquisition is no longer dependant on producing images to obtain exposure index values or image pixel variations and therefore no images are required. The measured dose values over the clinical kVp range are analysed for their agreement with the dose value at the calibrated dose set-point of the AEC system. The resulting set of data can be displayed on a variance table or graphed for a visual comparison.

9.1.1 Applicability of the AEC optimisation procedure

The procedure used relies on dose measurements taken at the plane of a CR cassette in a Bucky equipped with AEC. Implementation of the AEC optimisation can be carried out on almost any x-ray machine. The modern x-ray machine such as the Philips x-ray machine used to perform the tests for this thesis has the Bucky configuration as described in section 6.5 and presents no problems for the measurement of dose to the plane of the image medium. The measuring ion chamber can easily be placed in the Bucky tray and the whole assembly is manually moved into position. However in some machines the position of a cassette in the Bucky is controlled by automated motorised mechanisms. This type of mechanism is common for machines that

incorporate normal radiography with an image intensifier for performing fluoroscopy examinations. The extent of Bucky assembly movement in this type of mechanism is much greater than standard radiographic only systems. Placing an ion chamber in this type of Bucky arrangement severely compromises the physical integrity of the ion chamber and its attached cable as it is automatically drawn into the exposure position within the Bucky. Therefore the AEC test procedure to measure dose to the IP cannot be safely applied to this type of x-ray equipment.

The AEC optimisation procedure for CR described in section 5.2 relies on the ability to adjust the AEC control circuitry appropriately for the imaging medium. The AEC circuitry of older x-ray machines may not be adjustable or may require hardware changes to accommodate the requirements for CR. Some later AEC designs may be software controlled but may not have the adjustment range to accommodate CR response characteristics. Then there is a potential problem that the need for such a calibration may not be fully recognised because good quality images will be produced with CR, even when the AEC calibration is incorrect (Greig and Williams 2005).

9.2 The impact of a new AEC testing protocol on the working environment of the Medical Physicist

Before a new protocol for a process can be implemented successfully, some important questions about how it will integrate into the work program must be answered. These questions include but are not restricted to the following:

- Does it improve work flow?
- Does it simplify the process or does it add complexity?
- Is a complete or partial change of procedures required to implement the protocol?
- What training is necessary to achieve competence in the use of the new protocol?

When an AEC is optimally calibrated to match the response of an imaging medium the result is greater EI and dose consistency. There is also a greater level of consistency in image quality and noise response. However, while the experimental results provide the evidence of quantitative improvements in image quality and noise, they do not manifest themselves to a level which is quantifiable when viewing test images. This

has been confirmed by a blind study of clinical images randomly selected from a range of images and derived from exposures produced with and without AEC kVp optimisation. This result implies that no changes to clinical procedures or practices are required due to the introduction of the proposed AEC assessment protocol.

9.2.1 Test time reduction for AEC assessment using a dose alone protocol

A dose alone measurement protocol for AEC testing will substantially reduce the AEC functionality testing time for the Medical Physicist. The actual test time reduction will depend on the test mode currently employed by the Physicist and the combination of equipment at a site. Test procedures employed by other medical physicists groups may vary from those described for this thesis. Any variations from the described test procedures can have a direct impact on the AEC functionality test time. For example, the number of people involved in the test process and the choice of recording exposures on individual films compared to the rotating window image capture method will each have a direct influence on the time required to perform the test procedures. Table 9.1 illustrates the test sequence and test times at Christchurch Hospital for a conventional AEC functionality test sequence for a single Bucky. The testing sequence is divided into several operations or tasks to which the total test time is apportioned. Tasks marked with an asterisk are common to screen-film and CR based AEC setups.

It should be noted that the CR related times are for a Kodak CR system. Other CR systems such as Agfa allow a region of interest (ROI) to be selected on their image monitor and an image mean pixel value can be recorded from this. For this type of CR, the rotating lead window method of recording AEC exposures on a single IP referred to in section 3.6 could be used to good advantage to improve test efficiency.

The times shown are based on my own experience with AEC testing at the Hospital. Over three test sequences the average test time was 44 ± 10 minutes. The variability factor allows for the operational nuances of individual x-ray machine, test set-up time and unplanned delays that can arise in the normal run of a test sequence.

When a dose alone measurement AEC protocol is used the total test time for the Medical Physicist is 22 minutes, a reduction of 50% when compared to the normal AEC test time of 44 minutes. A single x-ray room can be equipped with two Buckys which implies a 44 minute time reduction per room. Since no image processing is

required the CR reader is always available for clinical use. This has a positive influence on the operational efficiency of the Radiology Department.

Task	Physicist's Time (min)		X-ray Machine Time (min)	Image Processor time	
	Film	CR	Film & CR	CR (Kodak)	Film
Basic test set-up (x-ray machine and test equipment, single Bucky) *	6	6	6	0	0
AEC test run including exposure data recording (22 exposures) *	11	11	11	0	0
Processing radiographic film (22 images- single film using the rotating exposure window technique)	5		0	0	5
Processing CR images (22 individual images for Kodak) and recording data.		22	0	44	0
Analysing images and recording data, analysing data :Radiographic film	8		0	0	0
Analysing data	5	5	0	0	0
Total times for normal testing (minutes)	30	44	17	44	5
Total time for dose only testing (minutes)	22	22	17	0	0

Table 9.1 Breakdown of AEC test sequence times for a single Bucky

The practical time savings made using the dose alone protocol will depend on individual test methods in current use which may differ from that described in this work.

9.3 General conclusions of thesis

This thesis has used a Kodak CR as an example of a digital imaging system. The work describes the test process required to assess the performance of current AECs to match the kVp response of a CR imaging medium. The result highlighted inaccuracies in the calibration of the AEC equipment at Christchurch Hospital. It showed that AECs could be calibrated with greater accuracy than could be attained using the supplied generic algorithms. The result not only showed that image exposure index values

achieved greater consistency under these conditions but also that measured AEC dose values were more consistent over the clinical kVp range.

The outcome of these tests was used to develop a new Medical Physics protocol for testing AEC functionality within the CR environment using just the measurement of AEC dose alone. The successful application of this protocol relies on the implementation of and adherence to stringent AEC set up procedures for all new and existing x-ray installations. The protocol requires optimisation of the AEC calibration to match the kVp characteristic of the imaging medium for each x-ray machine. Optimisation of AEC calibration implies consistent exposure index values over the clinical kVp range 60 kVp – 120 kVp. The dose variation over this kVp range should also be consistent around the set dose-point value of the AEC. The experimental results have shown that an 8% variation of dose about the dose set-point is achievable corresponding to range of ± 35 exposure index values. Accordingly a variation limit of twice the experimentally attained value would provide a reasonable limit of expectation for a test procedure to provide a method to assess the accuracy of AEC functionality.

The use of a dose alone measurement protocol for AEC testing still requires a regular qualitative assurance program to assess the accuracy of AEC functionality and to assure consistent imaging quality.

Doyle and Martin (1996) proposed a very similar procedure for determining AEC consistency. They are in concordance with this thesis that image receptor dose levels must change to reflect the variable kVp response characteristic of the receptor to obtain consistent image detector dose indices (equivalent to EI values used in this thesis). They also determined that the relative response of the detector dose indices at different tube potentials follows a similar pattern to the SNR and relates to the level of image quality. The SNR was defined as the mean pixel value divided by the standard deviation and taken from regions of interest of approximately 10 cm^2 drawn at the centre of each image. This concept was explored in section 8.4 of this thesis and resulted in similar findings. The fundamental difference between the procedures used by Doyle and Martin (1996) and this thesis is the analysis of image exposure indices to determine AEC consistency compared to optimizing image receptor dose values.

An alternative method of AEC optimization was proposed by Mazzocchi et al (2006). The method used the correlation of Exposure index readings and SNR. The SNR related to the optimal exposure index value at the image plate was used as the

reference value. The AEC system was thereafter calibrated in order to achieve that predefined SNR by means of the evaluated exposure index value. The parallel to this thesis is made by the relationship between optimal dose to the image plate and the consistency of image homogeneity determined from the recorded image pixel standard deviation values which are directly related to the calculation of SNR values.

9.4 Final Conclusions and future work

CR is now well established in the Christchurch Radiology Department and now direct radiology DR systems are beginning to appear in the workplace. The results obtained for this work are applicable only to the Kodak CR reader imaging environment. The results for other CR imaging systems or DR x-ray and imaging systems would require independent assessment based on their own unique mode of operation. This could be explored and confirmed in future work. However the principle remains that AECs are required to control patient doses and they require optimisation to match the response of their associated imaging system with the result that image consistency is maximised and image quality is optimised.

This thesis derives a process to achieve optimised kVp compensation for any AEC associated with any imaging medium which consequently enables the use of a test procedure which measures the consistency of dose to a CR IP to assess AEC functionality. There is no apparent significant clinical impact to normal radiographic practice due to the implementation of this process however it may provide benefits in operational efficiency with reductions in machine test times. In contrast to the subjectively variable nature of the measurement of image quality, the effects of the proposed AEC setup protocol on the measurements of EI, exposure dose and image noise are based in physics and produce quantifiable results. The test results show the benefits of achieving greater dose control consistency for AEC controlled exposures.

The Medical Physicist and Radiology Department will realise quantifiable efficiencies in both time and process management when using the measurement of dose alone measurement protocol to assess the functionality of AECs.

9.5 Formal Statement

I believe that the calibration of an AEC should provide consistent image quality. An AEC can be calibrated such that the dose to the image plate under varying conditions of kVp and absorber thickness is optimised for consistency. This dose can never be

absolutely consistent as long as the image medium has a non linear response to kVp. However it is the attainment of maximum consistency which makes it reasonable to accept the measurement of dose alone to be sufficient to indicate the state of an AEC's calibration. The test time to assess AEC performance can be considerably reduced when a dose alone measurement protocol is used. This is achieved because there is no requirement to expose and process an IP for each exposure of a full AEC test sequence of variable kVp, absorber thickness and density control.

END

References

AAPM (American Association of Physics in Medicine) 2002 *Acceptance testing and Quality control of photostimulable storage phosphor imaging systems report of task group #10* Draft Document

Birch, R. and Marshall M. 1979 Computation of Bremsstrahlung X-ray Spectra and Comparison with Spectra Measured with a Ge (Li) Detector. *Physics in Medicine and Biology* 24: 505

Bogucki, T. Trauernicht D. and Kocher T. 1995 Characteristics of a storage phosphor system or medical imaging *Kodak Health Sciences, Scientific Monograph 6*

Bradford, C. J. Peppler W. and Dobbins J. 1999 Performance characteristics of a Kodak computed radiography system. *Medical Physics* 26 (1): 27-37

Bushberg, J. Seibert J. Leidhold E. and Boone J. 2002 *The Essential Physics of Medical Imaging.* Second Edition. Lippincott Williams and Wilkins.

Christensen, E. Curry T. and Dowdey J. 1990 *Christensen's Physics of Diagnostic Radiology.* Fourth Edition. Lippincott Williams and Wilkins.

Christodoulou, E. Goodsitt M. Chan Heang-Ping and Hepburn T.2000 Phototimer setup for CR imaging. *Medical Physics* 27(12): 2652-2658

Cowan, A. Clarke O. Coleman N. Craven D. McArdle S. and Hay G 1992 *Leeds X-ray Test Object Instruction Manual.* The University of Leeds

Crawford. M and Brixner L. 1991 Photostimulable phosphors for x-ray imaging: applications and mechanism. *Journal of Luminescence* 37: 48 - 49

Doyle, P. Gentle D. and Martin C.J. 2005 Optimising automatic exposure control in computed radiography and the impact on patient dose. *Radiation Protection Dosimetry*: 14:236-239

Doyle, P. and Martin C.J. 2006 Calibrating automatic exposure control devices for digital radiography. *Physics in Medicine and Biology* 51: 5475-5485

Fetterly, K. and Hangiandreou N. 2001 Effects of x-ray spectra on the DQE of a computed radiography system. *Medical Physics* 28 (2): 241-249

Goldman, L. and Yester M. 2004 Specifications, Performance Evaluation and Quality Assurance of Radiographic and Fluoroscopic Systems in the Digital Era *Medical Physics Monograph* 30. American Association of Physicists in Medicine Summer School Proceedings

Grieg, L. and Williams J. 2005 *AEC Calibration with CR systems'* Oral presentation British Institute of Radiology Scientific meeting, Department of Medical Physics, Royal Infirmary of Edinburgh, NHS Lothian. <www.mph.ed.ac.uk/nhs/downloads/CR0205Abs2.pdf> Accessed November 18, 2005

Hale, J. 1989 Routine calibration of automatic exposure control systems for diagnostic *x*-ray machines: A 5yr report. *Health Physics* 57 (6): 1021-1024.

Heggie, J.C.P. Liddel N.A. and Maher K.P. 2001 *Applied Imaging Technology* Fourth Edition. St Vincent's Hospital.

Hendee, W. 1979 *Medical Radiation Physics* Second Edition. Year Book Medical Publishers, Chicago

Huda, W. 1997 Relative speeds of Kodak computed radiography phosphors and screen-film systems. *Medical Physics* 24 (10): 1621-1628

Hunt, A. and Plain S. 1993 A simple solution to the problems of testing automatic exposure control in diagnostic radiology. *The British Journal of Radiology* 66: 360-362

ICRU [International Commission on Radiation Units and Measurements] 1980 *Radiation Quantities and Units* Report 33. Washington DC

IPEM [Institute of Physics and Engineering in Medicine] 2005 *Recommended Standards for the Routine Performance Testing of Diagnostic X-ray Imaging Systems.* Report 91. York. Fairmount House

Lu, Z. Nickoloff E. So J. and Dutta A. 2002 Comparison of computed radiography and film/screen combination using a contrast-detail phantom. *Journal of Applied Clinical Medical Physics:* Vol 4 (1): 91-98

Mazzocchi, S. Belli G. Busoni S. Gori C. Menchi I. Salucci P. and Taddeucci A. 2006 AEC Set-up Optimisation with Computed Radiography. *Radiation Protection Dosimetry:* 117(1-3): 169-173

Mould R.F. 1995 The early history of x-ray diagnosis with emphasis on the contributions of physics 1895-1915. *Physics in Medicine and Biology* 40: 1741-1787

NIST [National Institute of Standards and Technology] x-ray mass attenuation tables U.S. Department of Commerce <http://physics.nist.gov/Divisions/Div846/div846.html> Accessed March 09, 2004

Newing, A. 1999 Light visible and invisible and its medical applications. *British Journal of Radiology* 74: 212

Nowotny, R.1998 *XMuDat: Photon attenuation data on PC IAEA* [International Atomic Energy Agency] < http://www-nds.iaea.org/reports/nds-195.htm> Accessed 2 February 2005

NRL [National Radiation Laboratory] C5 1994 *Code of safe practice for the use of x-rays in medical diagnosis.* Ministry of Health Christchurch New Zealand.

Nyquist, H. 1928 Certain Topics in Telegraph Transmission Theory. *Transactions of the AIEE(American Institute of Electrical Engineers)* 47: 617-644.

Orand, M. 2004 '*Cost Analysis: Film vs. PACS'* <www.radiologytoday.net/archive/rt_051004p38.shtml> Accessed October 06, 2003

Rowlands, J.A 2002 The Physics of Computed Radiography. *Physics in Medicine and Biology* 47:R123-R166.

Seggern, H. 1999 Photostimulable x-ray storage phosphors: a review of present understanding. *Brazilian Journal of Physics* 29 (2): 254-268

Seibert J. A. 2003 *Digital radiography 2003 an overview* (Power point presentation) UC Davis Department of Radiography Sacramento, California.

Seibert J. A 2004 Computed Radiography Technology. *Department of Radiology University of California Davis Medical Centre*: Cited In: Goldmann LW, Yester MV, eds. *Specifications, performance evaluation, and quality assurance of radiographic and fluoroscopic systems in the digital era.* Madison, WI: Medical Physics Publishing, 2004:153 -175

Stirling, G. 'Specgen' computer program for analysing radiographic spectrum NRL(National Radiation Laboratory), Christchurch New Zealand.

Takahashi, K. 2002 Progress in science and technology on photostimulable BaFX: Eu^{2+} (X=Cl, Br, I) and imaging plates. *Journal of Luminescence* 100:307-315

University of Chicago Department of Radiology 2004 *The Early Years,* University of Chicago Biological Sciences Division, Chicago. <www.radiology.uchicago.edu/earlyyears.htm> Accessed 20 July 2005

Van Loon, R. and Van Tiggelen R.2004 *History of dosimetry in radiology and early radiotherapy* <www.radiology-museum.be/English/Collection/RadioprotectHist.asp> Accessed 20 July 2005

Wilkinson, L.E. and Heggie J.C.P. 1997 Determination of Correct AEC Function with Computed Radiography Cassettes. *Australian Physical and Engineering Sciences in Medicine* 20 (3):186-191

Workman, A. and Cowan A. 1993 Signal, Noise and SNR transfer properties of computed radiography. *Physics in Medicine and Biology* 38:1789-1808

Yaffe, M. and Rowlands J. 1997 X-ray detectors for digital radiography. *Physics in Medicine and Biology* 42:1-39.

.

Index of Figures

Index of Tables

Acronyms

AEC	Automatic exposure control
ALARA	As low as reasonably achievable
C	Coulomb (S.I) unit of electrical charge)
CCD	Cold cathode detector (Photoelectric detector)
CGS	Centimetre, gram, second (System of measuring units)
CMOS	Complimentary metal oxide (semiconductor type)
CR	Computed Radiography
CRT	Cathode ray tube
CT	Computed Tomography (CT scanner)
DICOM	Digital Imaging and Communications in Medicine
DR	Digital Radiography
EI	Exposure Index
Esu	Electrostatic unit (CGS system unit of electrical charge)
GSDF	Greyscale Standard Display Function
Gy	Gray (S.I Unit of radiation)
IAEA	International Atomic Energy Agency
ICRU	International commission on Radiation Units
IP	Imaging plate
ISO	International Standards Organisation
KeV	Kiloelectron volts
Kgs	Kilograms
kVp	Kilovoltage Peak

LCD	Liquid crystal display
MRT	Medical Radiation Technologist (Radiographer)
NRL	National Radiation Laboratory
OD	Optical Density
PACS	Picture Archiving and Communications System
PEP	Patient Equivalent Phantom
PMT	Photomultiplier Tube
PSD	Pixel standard deviation
PSL	Photostimulated luminescence
PSP	Photostimulable Phosphor
QHP	Qualified Health Physicist
OSI	Open System Interconnection
R	Roentgen (Traditional unit of radiation)
ROI	Region of interest
ROP	Remote operators panel (Kodak)
S.I	International system of measuring units
S.I.D	Source to image distance
SNR	Signal to noise ratio
TFT	Thin film transistor (technology used in flat panel imaging arrays)